Supersymmetric radiative corrections on $\mu - \tau$ neutrino refraction including possible R-parity breaking interactions

J. Gava*

Institut de Physique Nucléaire, CNRS/IN2P3 UMR 8608 and Université Paris-Sud 11, Bât. 100, F-91406 Orsay cedex, France

C.-C. Jean-Louis†

Laboratoire de Physique Théorique, CNRS UMR 8627, Bât. 210, Université Paris-Sud 11, 91405 Orsay Cedex, France

(Received 22 July 2009; published 22 January 2010)

In this paper we investigate the one-loop radiative corrections to the neutrino indices of refraction from supersymmetric models. We consider the next-to-minimal supersymmetric extension of the standard model which happens to be a better supersymmetric candidate than the minimal supersymmetric standard model for both theoretical and experimental reasons. We scan the relevant supersymmetry parameters and identify regions in the parameter space which yield interesting values for $V_{\mu\tau}$. If R-parity is broken there are significant differences between the minimal supersymmetric standard model and next-to-minimal supersymmetric extension of the standard model contributions contrary to the R-parity conserved case. Finally, for a nonzero CP-violating phase, we show analytically that the presence of $V_{\mu\tau}$ will explicitly imply CP-violation effects on the supernova electron (anti)neutrino fluxes.

DOI: 10.1103/PhysRevD.81.013003 PACS numbers: 14.60.Pq, 11.30.Fs, 11.30.Pb, 97.60.Bw

I. INTRODUCTION

The charged-current interaction between neutrinos and their associated leptons present in the medium give an effective matter potential which can lead to a resonant flavour conversion called the Mikheyev-Smirnov-Wolfenstein effect [1,2]. Such behavior elegantly solves the solar neutrino deficit problem first pointed out by pioneering experiment of R. Davis in the 1960s [3]. This phenomenon is of crucial importance for the propagation of neutrinos in the supernova environment whose flux detection could yield precious information concerning the dynamics of the density profile or fundamental neutrinos properties like the hierarchy or the value of the third mixing angle θ_{13}. In supernovae, depending on the mass hierarchy, the electron neutrino may encounter one or two resonances via a charged current, while the muon or tau neutrinos will only interact via a neutral current indistinguishable at the tree level in the standard model (SM). Indeed, due to the absence of a muon or tau particle in such an environment, coherent forward scattering may only intervene via neutral current to which all flavors are sensitive. In the case of a neutral medium [4,5], the electromagnetic corrections [i.e $O(\alpha)$] were shown to be negligible. Considering that matter interaction can also be seen as a neutrino index of refraction [6,7], Botella *et al.* [8], proved that differences at one loop in the neutrino index of refraction could arise for muon and tau neutrinos at order $O(\frac{\alpha}{\pi \sin^2\theta_W} \frac{m_\tau^2}{M_W^2})$. Later, supersymmetric radiative corrections, in the case of the minimal supersymmetric model (MSSM) have been partially calculated [9] showing that it could give potentially much larger radiative effects than in the standard model. It is interesting to note that such radiative corrections have been for a longtime considered as negligible or without observable consequences for the supernova environment.[1] Such consideration was probably true when not taking into account the neutrino-neutrino interaction which has dramatically changed the vision we have of neutrino propagating in an exploding star and which has gone through an intense investigation [11–35]. Actually few papers have shown the importance of the one-loop correction in addition with the neutrino-neutrino interaction. First it has been shown that for early time after post-bounce when the matter density is very high, neutrinos can encounter the $\mu - \tau$ resonance and possibly modify the ν_e flux [27,29]. Unfortunately, it has also been shown that in such a case the high density in addition with a multiangle neutrino-neutrino interaction would make those effects vanish [33]. Besides those works, only two papers[2] [31,36], have shown the importance of $V_{\mu\tau}$ via the influence of the CP-violating phase δ contained in the Maki-Nakagawa-Sakata-Pontecorvo (MNSP) matrix and whose value is still unknown. Such a term induces the effects of a nonzero CP-violating phase on the electron neutrino fluxes inside and outside the supernova.

The goal of this paper is to calculate such corrections in the supersymmetry (SUSY) framework with and without R-parity breaking interactions. We consider a more general approach than the one done in [9]. First, we complete the

*gava@ipno.in2p3.fr
†charles.jean-louis@th.u-psud.fr

[1]Note that in [10] it has been first observed that $V_{\mu\tau}$ can have some important effects on the neutrino states if the ν_μ and ν_τ fluxes are different.

[2]In [29], it was noted that the CP-violating phase could sensibly influence the μ and τ neutrino flavor.

calculations of the possible diagrams present in the MSSM with respect to [9] where only partial corrections have been made. Second, we actually consider the next-to-minimal supersymmetric extension of the standard model (NMSSM),[3] which is a more general model and allows us to solve the μ problem of the MSSM. Moreover, the NMSSM is less constrained experimentally as discussed in the next section. For all these reasons, it is a more promising supersymmetric model than the MSSM, and presents a wider space of parameters which logically imply possible larger radiative corrections. Finally, our model is self-consistent insofar as some R-parity breaking terms considered here provide a scenario able to generate neutrino masses at the tree level.

The paper is organized as follows: Sec. II introduces the theoretical framework where we briefly remember how to calculate radiative corrections in this context and more importantly where we introduce the supersymmetric framework. The corrections with R-parity conservation are calculated in Sec. III and Sec. IV is dedicated to the case where the R-parity is broken. Before concluding, we explicitly demonstrate in Sec. V the influence of $V_{\mu\tau}$ on the ν_e flux when the CP-violating phase is nonzero and we discuss the results in Sec. VI.

II. THEORETICAL FRAMEWORK

A. The calculations of the radiative corrections

Neutrinos interaction through matter can be described using indices of refraction and in this case, the evolution equation of neutrinos with matter, omitting the neutrino-neutrino interaction is

$$i\frac{d}{dt}\begin{pmatrix}\nu_e\\ \nu_\mu\\ \nu_\tau\end{pmatrix} = \left[\frac{1}{2p_\nu}U\begin{pmatrix}\Delta m^2_{12} & 0 & 0\\ 0 & 0 & 0\\ 0 & 0 & \Delta m^2_{32}\end{pmatrix}U^\dagger - p_\nu\begin{pmatrix}\Delta n_{e\mu} & 0 & 0\\ 0 & 0 & 0\\ 0 & 0 & \Delta n_{\tau\mu}\end{pmatrix}\right]\begin{pmatrix}\nu_e\\ \nu_\mu\\ \nu_\tau\end{pmatrix}, \quad (1)$$

where, p_ν is the neutrino momentum, $\Delta m^2_{ij} \equiv m^2_{\nu_i} - m^2_{\nu_j}$, $\Delta n_{\alpha\beta} \equiv n_{\nu_\alpha} - n_{\nu_\beta}$, and U is the MNSP matrix

$$U = T_{23}T_{13}T_{12} = \begin{pmatrix}1 & 0 & 0\\ 0 & c_{23} & s_{23}\\ 0 & -s_{23} & c_{23}\end{pmatrix}\begin{pmatrix}c_{13} & 0 & s_{13}e^{-i\delta}\\ 0 & 1 & 0\\ -s_{13}e^{i\delta} & 0 & c_{13}\end{pmatrix} \times \begin{pmatrix}c_{12} & s_{12} & 0\\ -s_{12} & c_{12} & 0\\ 0 & 0 & 1\end{pmatrix}, \quad (2)$$

where $c_{ij} = \cos\theta_{ij}$ ($s_{ij} = \sin\theta_{ij}$) with θ_{12}, θ_{23}, and θ_{13} the three neutrino mixing angles. The presence of a Dirac δ phase in Eq. (2) renders U complex and introduces a difference between matter and antimatter. To size the effect of such a radiative correction on the neutrino propagation, we study the one-loop effect on the scattering amplitude matrix which describes the interaction of neutrinos with matter:

$$M(\nu_\ell f \to \nu_\ell f) = -i\frac{G_F}{\sqrt{2}}\bar{\nu}_\ell\gamma^\rho(1-\gamma_5)\nu_\ell \times \bar{f}\gamma_\rho(C^V_{\nu_\ell f} + C^A_{\nu_\ell f}\gamma_5)f. \quad (3)$$

In the calculations we will use the same approximations as in [8,9] i.e, neutrinos are propagating though an unpolarized medium at rest. Consequently, the neutrino index of refraction can be written as

$$p_\nu(n_{\nu_\ell} - 1) = -\sqrt{2}G_F\sum_{f=u,d,e} C^V_{\nu_\ell f}N_f, \quad (4)$$

where N_f is the number density of fermion f in the medium. Therefore, the interesting parameter to study in order to size the radiative correction to matter interaction is $C^V_{\nu_\ell f}$ which is defined at the tree level by

$$C^V_{\nu_\ell f} = T_3(f_L) - 2Q_f\sin^2\theta_W + \delta_{\ell f}, \quad (5)$$

with $\sin^2\theta_W \equiv 1 - m^2_W/m^2_Z \simeq 0.23$, while Q_f and $T_3(f_L)$ are, respectively, the electric charge and the third component of the weak isospin of the fermion f_L. To parametrize the loop corrections to $C^V_{\nu_\ell f}$ Botella *et al.* [8] have defined in some kind of an arbitrary but convenient way a new $C^V_{\nu_\ell f}$ by

$$C^V_{\nu_\ell f} = \rho^{\nu_\ell f}T_3(f_L) - 2Q_f\lambda^{\nu_\ell f}s^2_W. \quad (6)$$

for $f \neq \ell$ where the $\rho^{\nu_\ell f}$ includes the f-dependent (box) diagrams' contributions. Since the $\lambda^{\nu_\ell f}$ are independent of f, in a electrically neutral medium, they will not contribute to $\Delta n_{\tau\mu}$. Consequently, $\Delta n_{\tau\mu}$ will only be sensitive to $\Delta\rho^f \equiv \rho^{\nu_\tau f} - \rho^{\nu_\mu f}$. Note that we are only interested in the difference between n_{ν_μ} and n_{ν_τ} indices of refraction because the loop correction to $\Delta n_{e\mu} = -\sqrt{2}G_F N_e/p_\nu$ will be negligible since electron neutrinos already encounter charged-current interactions with matter. In the standard model, the corrections have been calculated and are found to be small:

$$-p_\nu\Delta n_{\tau\mu} = V_{\mu\tau} = \varepsilon V_e \simeq 5.4\times 10^{-5}V_e, \quad (7)$$

where $V_{\mu\tau}$ is the effective matter potential to tau neutrinos due to one-loop corrections and ε the ratio between the $V_{\mu\tau}$ and V_e which yields the size of the loop correction in comparison with the charged-current matter potential for electron neutrinos V_e.

[3]Note that the NMSSM contains the phenomenology of the MSSM, as it is going to be described in the following section.

B. The supersymmetric framework

The most significant theoretical issues of the standard model are the hierarchy problem for the Higgs mass and the nonunification of the gauge couplings. Supersymmetry allows us to address these problems and is an attractive candidate for new physics beyond the standard model. In this theory a supersymmetric particle called LSP (lightest supersymmetric particle) is a natural candidate for dark matter. Among various supersymmetric models the most extensively studied is the MSSM.

The MSSM contains the minimum number of fields to describe the known standard model particles and their superpartners. To SM fermionic fields (leptons, quarks), we have supersymmetric scalar fields (sleptons, squarks) associated. Concerning SM vector bosons [$U(1)_Y$, $SU(2)_L$, $SU(3)_C$ gauge bosons], fermionic fields called gauginos (bino, winos, gluinos) are associated to [37]. Finally, we have fermionic fields called higgsinos associated to Higgs bosons. Higgsinos and gauginos will mix to generate neutralinos and charginos.

We call superpotential all the renormalizable products of chiral superfields in a given supersymmetric model where a chiral superfield is a multiplet which contains a scalar field and a fermionic field. The MSSM's superpotential is

$$W_{\mathrm{MSSM}} = h_t\hat{Q}\cdot\hat{H}_u\hat{T}_R^c - h_b\hat{Q}\cdot\hat{H}_d\hat{B}_R^c - h_\tau\hat{L}\cdot\hat{H}_d\hat{L}_R^c + \mu\hat{H}_u\cdot\hat{H}_d \tag{8}$$

where $\hat{H}_u$, $\hat{Q}\ldots$ are chiral superfields. The fermionic part of the supersymmetric Lagrangian is obtained through a procedure where the superfields of the superpotential are expanded in terms of component fields and then the superspace coordinates of the result are integrated out:

$$\begin{aligned}\mathcal{L}_{\mathrm{MSSM}} = {}& h_t\psi_Q\cdot H_u\psi_{T_R^c} - h_b\psi_Q\cdot H_d\psi_{B_R^c}\\ &- h_\tau\psi_L\cdot H_d\psi_{L_R^c} + \mu\psi_{H_u}\cdot\psi_{H_d}\\ &+\ldots(+\mathrm{H.c.}).\end{aligned} \tag{9}$$

In supersymmetry, we need two Higgs bosons to give masses to the other particles.

Despite its simplicity, there are two unexplained hierarchies, within the MSSM:

(i) the so-called μ problem [38]. It arises from the presence of a mass μ term for the Higgs fields in the superpotential. The only two theoretical natural values for this parameter are either zero or the Planck energy scale. However, we need $\mu \gtrsim 100$ GeV to satisfy LEP constraints on the chargino masses and $\mu \lesssim M_{\mathrm{SUSY}}$ for a destabilization of the Higgs potential in order to have nonvanishing vacuum expectation value (v.e.v.) for the scalar Higgs fields ($<H_{u,d}> \neq 0$).

(ii) The other hierarchy with an unknown origin is the one existing between the small neutrino masses (smaller than the eV scale) and the electroweak symmetry breaking scale (~ 100 GeV).

In this paper, our framework is the NMSSM [39]. This model provides an elegant solution to the μ problem via the introduction of a new gauge-singlet superfield $\hat{S}$ that acquires naturally a v.e.v. x of the order of the supersymmetry breaking scale, generating an effective μ parameter ($\lambda x = \mu_{\mathrm{eff}}$) of order of the electroweak scale. Furthermore, if we break a discrete symmetry called R-parity we can explain in the NMSSM framework the second hierarchy by generating two neutrino masses at the tree level [40] as we will see below.

The NMSSM's superpotential is

$$\begin{aligned}W_{\mathrm{NMSSM}} = {}& h_t\hat{Q}\cdot\hat{H}_u\hat{T}_R^c - h_b\hat{Q}\cdot\hat{H}_d\hat{B}_R^c - h_\tau\hat{L}\cdot\hat{H}_d\hat{L}_R^c\\ &+ \lambda\hat{S}\hat{H}_u\cdot\hat{H}_d + \frac{\kappa}{3}\hat{S}^3.\end{aligned} \tag{10}$$

Then, the fermionic part of the NMSSM Lagrangian is

$$\begin{aligned}\mathcal{L}_{\mathrm{NMSSM}} = {}& h_t\psi_Q\cdot H_u\psi_{T_R^c} - h_b\psi_Q\cdot H_d\psi_{B_R^c}\\ &- h_\tau\psi_L\cdot H_d\psi_{L_R^c} + \lambda S\psi_{H_u}\cdot\psi_{H_d}\\ &+ \kappa S\psi_S\psi_S + \ldots(+\mathrm{H.c.}).\end{aligned} \tag{11}$$

The NMSSM contains the following particles:

(i) Standard model fermions and their left and right scalar supersymmetric partners (sfermions)
(ii) Standard model gauge bosons
(iii) 3 neutral scalar Higgs (h_1, h_2, h_3)
(iv) 2 neutral pseudoscalar Higgs (a_1, a_2)
(v) 1 charged Higgs ($H^\pm$)
(vi) 2 charginos ($\chi^\pm_{1,2}$) originally from mixing between charged fermionic superpartners of the gauge bosons (gauginos) and charged fermionic superpartners of Higgs bosons (higgsinos)
(vii) 5 neutralinos ($\chi^0_{1\ldots5}$) of which the lightest, LSP, is generally stable and is then a natural candidate for dark matter. They come from the mixing between neutral gauginos and neutral higgsinos.

The NMSSM phenomenology contains the MSSM phenomenology if we take $\lambda\to0$, $\kappa\to0$ by keeping μ_{eff} of the order of M_W. However, the NMSSM is less constrained experimentally than the MSSM. In particular, the theoretical value of the lightest scalar Higgs mass in the NMSSM is above the MSSM one. It can go up to 150 GeV for small values of $\tan\beta$ while the LEP experimental constraints on the SM-like Higgs mass give $m_{h_1} \gtrsim 114$ GeV. Furthermore, there exist new decay channels for h_1 in two pseudoscalar Higgs which allow us to relax the experimental lower bound on m_{h_1}. Consequently, in the NMSSM, for some regions of the parameters space, this lower bound can be $m_{h_1} \gtrsim 90$ GeV.

Experimental limits on supersymmetric particle masses obviously show that SUSY has to be broken. Thus, the supersymmetric particle masses will be different from standard model particle masses. The soft SUSY breaking terms in the NMSSM are

(a) mass terms for scalar particles:

$$m_{H_u}^2|H_u|^2 + m_{H_d}^2|H_d|^2 + m_S^2|S|^2 + m_{Q_3}^2|Q_3|^2 + m_{\tilde{t}_R}^2|T_R|^2 + m_{\tilde{b}_R}^2|B_R|^2 + m_{L_3}^2|L_3|^2 + m_{\tilde{\tau}_R}^2|L_R|^2 + \ldots$$

where all the fields are scalar fields,

(b) mass terms for gauginos:

$$\tfrac{1}{2}M_1\lambda_1\lambda_1 + \tfrac{1}{2}M_2\vec{\lambda}_2\cdot\vec{\lambda}_2 + \tfrac{1}{2}M_3\vec{\lambda}_3\cdot\vec{\lambda}_3,$$

(c) soft terms associated to the superpotential:

$$\lambda A_\lambda S H_u \cdot H_d + \frac{\kappa}{3}A_\kappa S^3 + h_t A_t Q\cdot H_u T_R^c - h_b A_b Q \cdot H_d B_R^c - h_\tau A_\tau L\cdot H_d L_R^c + \ldots(+\text{H.c.}),$$

where all fields are scalar fields.

III. R-PARITY CONSERVED SUSY CORRECTIONS

In supersymmetry, one usually considers all sfermions to be exactly degenerate at the GUT scale, and obtain their low-energy splittings from the renormalization group evolution of the soft parameters and from terms arising after the electroweak symmetry breaking. In this way, although squarks become significantly split from sleptons, the splittings among the masses of different slepton generations are only due to the small τ-Yukawa coupling. This usually implies that $m_{\tilde{\tau}}^2 - m_{\tilde{\mu}}^2$ is $O(m_\tau^2)$, and hence the radiative effects on the $\nu_{\mu,\tau}$ indices of refraction are, in this case, not larger than the standard model ones. In the following, we shall consider a large $\tilde{\tau}_L - \tilde{\tau}_R$ mixing. This occurs for large values of the effective μ parameter and $\tan\beta$, or for large values of the parameter A of the trilinear soft terms, in which case the splitting can be $O[m_\tau(A_\tau + \mu_{\text{eff}}\tan\beta)]$ as we can see below. $\tan\beta$ is the ratio v_u/v_d where v_u and v_d are the v.e.v. of the scalar Higgs fields H_u and H_d.

We give here the stau and smuon mass-squared matrices where we neglect splittings due to D terms among charged and neutral sleptons or among $\tilde{\ell}_L$ and $\tilde{\ell}_R$. The diagonal terms are, respectively, the $\tilde{\ell}_R$ and $\tilde{\ell}_L$ mass-squared terms.

For tau sleptons:

$$\mathcal{M}_{\tilde{\tau}}^2 = \begin{pmatrix} m_\tau^2 + m_{\tilde{\tau}_R}^2 & m_\tau(A_\tau + \mu_{\text{eff}}\tan\beta) \\ m_\tau(A_\tau + \mu_{\text{eff}}\tan\beta) & m_\tau^2 + m_{L_3}^2 \end{pmatrix}, \tag{12}$$

and for muon sleptons:

$$\mathcal{M}_{\tilde{\mu}}^2 = \begin{pmatrix} m_\mu^2 + m_{\tilde{\mu}_R}^2 & m_\mu(A_\mu + \mu_{\text{eff}}\tan\beta) \\ m_\mu(A_\mu + \mu_{\text{eff}}\tan\beta) & m_\mu^2 + m_{L_2}^2 \end{pmatrix}, \tag{13}$$

where

(i) $m_{\tilde{\tau}_R}^2$, $m_{\tilde{\mu}_R}^2$, $m_{L_3}^2$ and $m_{L_2}^2$ are of the order of $M_{\text{susy}}^2 \sim 0.1 - 1\ \text{TeV}^2$,

(ii) $(A_\tau + \mu_{\text{eff}}\tan\beta)$, $(A_\mu + \mu_{\text{eff}}\tan\beta)$ are of the order of M_{susy},

(iii) $m_\tau = 1.8$ GeV, $m_\mu = 105$ MeV.

In the 2nd generation case, we can neglect the mixing between $\tilde{\mu}_R$ and $\tilde{\mu}_L$ because the off-diagonal terms are negligible with respect to the diagonal terms. But in the third generation, we have to consider $\tilde{\tau}_1$, $\tilde{\tau}_2$ instead of $\tilde{\tau}_R$, $\tilde{\tau}_L$.

The SUSY contribution to $\Delta n_{\tau\mu}$ can then be larger than the standard model one.

In the following, to calculate the loop diagrams contributions we will use the dimensional regularization method and the vanishing external legs approximation [8,9] which turns out to be legitimate because of the low masses and energy of the fermions with respect to the electroweak (M_W) and SUSY (M_{SUSY}) breaking scales. When one does not use this approximation, the loop integrals needed to perform will have several different mass scales. Such calculations are much more complicated and need advanced mathematical methods as in [41]. In this framework, some specific functions will appear:

(i) For the self-energies and the penguin:

$$H_0(x,y) = \sqrt{xy}\left[\frac{x\ln x}{(x-y)(x-1)} + (x\leftrightarrow y)\right],$$

$$G_0(x,y) = \left[\frac{x^2\ln x}{(x-y)(x-1)} + (x\leftrightarrow y)\right].$$

(ii) For the box diagrams:

$$H'(x,y,z) = \sqrt{xy}\left[\frac{x\ln x}{(x-y)(x-z)(x-1)} + \frac{y\ln y}{(y-x)(y-z)(y-1)} + \frac{z\ln z}{(z-x)(z-y)(z-1)}\right],$$

$$G'(x,y,z) = \frac{x^2\ln x}{(x-y)(x-z)(x-1)} + \frac{y^2\ln y}{(y-x)(y-z)(y-1)} + \frac{z^2\ln z}{(z-x)(z-y)(z-1)}.$$

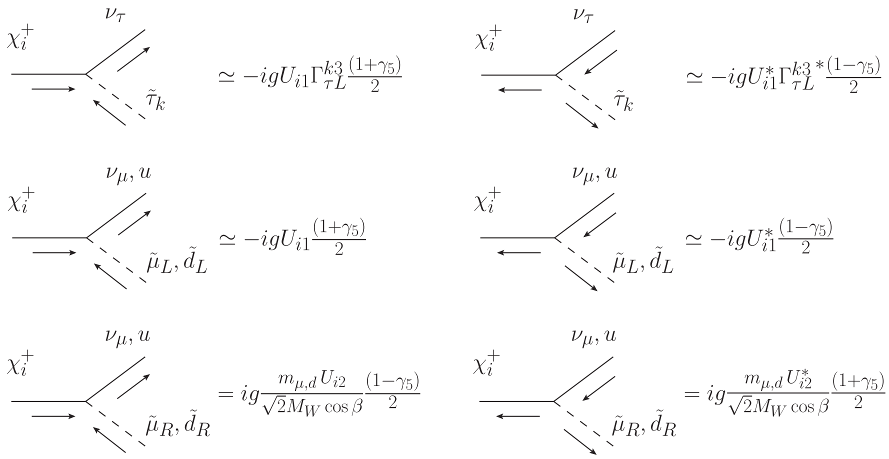

FIG. 1. R-parity conserved vertices involving charginos and up fermions.

A. Vertices

Following the notation of [42,43], we denote by N_{ij} by $\chi_i^0 \equiv N_{ij}\tilde{\Psi}_j$ where $\tilde{\Psi}^T = (\tilde{B}, \tilde{W}_3, \tilde{h}_u, \tilde{h}_d, \tilde{s})$, U and V are the 2×2 matrices required for the diagonalization of the chargino mass matrix.

We see in Figs. 1 and 2 that vertices between chargino χ_i^+, a fermion f, and the right scalar partner $\tilde{f}_R$ are negligible with respect to vertices between chargino χ_i^+, a fermion f, and the left scalar partner $\tilde{f}_L$ because $\frac{m_f}{M_W} \ll 1$ for $f \equiv \mu$, u, d. We will neglect the loops including the primary vertices below.

The coupling of one neutralino χ_i^0 (cf. 3) to one fermion and the associated left (right) scalar partner $G_{fL(R)}^j$ is

$$G_{fL}^j = Q_f \sin\theta_W N_{j1}^* + \frac{c_L^f}{\cos\theta_W} N_{j2}^*,$$

where $f \equiv \nu$, e, u, d;

$$G_{fR}^j = \mathrm{sign}(m_{\chi_j^0})\left[Q_f \sin\theta_W N_{j1} + \frac{c_R^f}{\cos\theta_W} N_{j2}\right],$$

where $f \equiv e$, u, d.

The coupling of left (right) scalar partners to the Z^0 boson is

$$c_{L(R)}^f = T_3(f_{L(R)}) - Q_f \sin^2\theta_W.$$

The coupling of scalar partners in their mass basis to the Z^0 boson [44] is

$$c_{fM}^{kj} = T_3(f)\sum_{i=1}^{3}\Gamma_{fL}^{ki}\Gamma_{fL}^{ji*} - Q_f \sin^2\theta_W \delta^{kh},$$

where $\tilde{\tau}_L = \Gamma_{\tau L}^{k3}\tilde{\tau}_k$. The coupling of charginos to the Z^0 boson [44,45], is

$$\mathcal{O}'^{L}_{ij} = -V_{i1}V_{j1}^* - \tfrac{1}{2}V_{i2}V_{j2}^* + \delta_{ij}\sin^2\theta_W,$$

and

$$\mathcal{O}'^{R}_{ij} = -U_{i1}U_{j1}^* - \tfrac{1}{2}U_{i2}U_{j2}^* + \delta_{ij}\sin^2\theta_W.$$

We will assume below that all the parameters are real.

B. Self-energy diagrams

The computation of the supersymmetric contribution to $\Delta\rho$ requires the evaluation of the Feynman diagrams.

The self-energy, penguin and box contributions to $\Delta\rho^f$ can be written as

$$\Delta\rho^f = \Delta\rho_p + \frac{\Delta\rho_{\mathrm{box}}^f}{T_3(f_L)}.$$

We consider here the contributions to neutrino and antineutrino scattering involving self-energy diagrams.

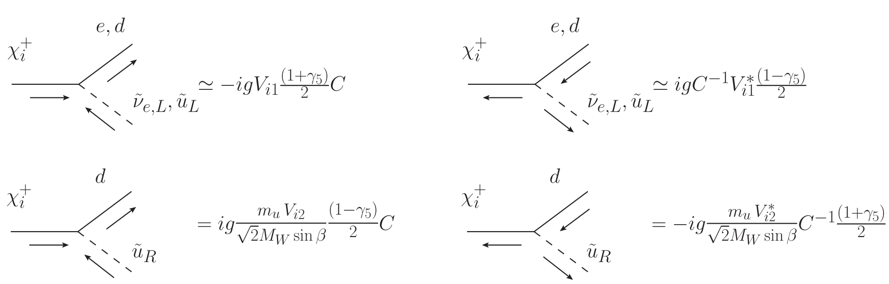

FIG. 2. R-parity conserved vertices involving charginos and down fermions.

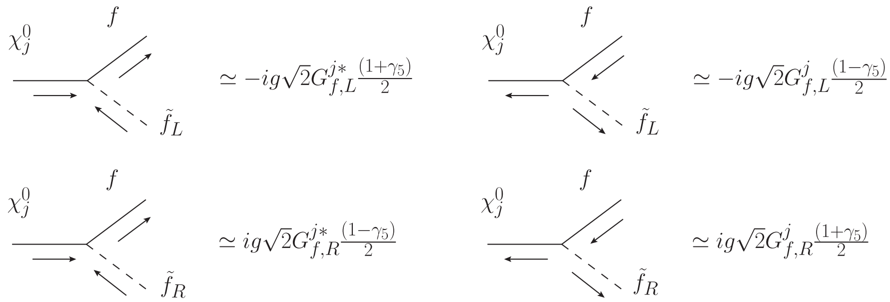

FIG. 3. R-parity conserved vertices involving neutralinos, fermions, and associated sfermions.

The first contribution implies a slepton-chargino loop [Fig. 5(a)]. We diagonalize the stau mass matrix and use the vertices of Fig. 1. We neglect the $\tilde{\mu}_R$ contribution;

$$\Delta\rho^{\tilde{\ell}}(\Sigma) = -\frac{\alpha_W}{8\pi}\sum_{j=1}^{2}U_{j1}^2\bigg[\sum_{k=1}^{2}\Gamma_{\tau L}^{k32}\bigg\{G_0(X_{\chi_j^+\tilde{\tau}_k},1)+\ln\frac{m_{\tilde{\tau}_k}^2}{\mu^2}\bigg\} - \bigg\{G_0(X_{\chi_j^+\tilde{\mu}_L},1)+\ln\frac{m_{\tilde{\mu}_L}^2}{\mu^2}\bigg\}\bigg], \tag{14}$$

where $X_{ab}=\frac{m_a^2}{m_b^2}$. Then, we have a neutralino-sneutrino loop [Fig. 6(c)];

$$\Delta\rho^{\tilde{\nu}}(\Sigma) = -\frac{\alpha_W}{4\pi}\sum_{j=1}^{5}G_{\nu L}^{j2}\bigg\{G_0(X_{\chi_j^0\tilde{\nu}_{\tau_L}},1) + \ln\frac{m_{\tilde{\nu}_{\tau_L}}^2}{\mu^2} - (\tilde{\nu}_{\tau_L}\to\tilde{\nu}_{\mu_L})\bigg\}. \tag{15}$$

C. Penguin diagrams

We consider here the contributions to (anti)neutrino scattering involving penguins. We use the vertices of Fig. 4.

$\Delta\rho_p(\tilde{\ell})$ implies a chargino-slepton loop in which the slepton couples to the Z^0 boson [Fig. 5(e)]. In $\Delta\rho_p(\chi^+)$, the chargino couples to the Z^0 boson [Fig. 5(c)]. $\Delta\rho_p^L(\tilde{\nu})$ implies a neutralino-sneutrino loop in which the sneutrino couples to the Z^0 boson [Fig. 6(a)] and in $\Delta\rho_p^L(\chi^0)$ the neutralino couples to the Z^0 boson [Fig. 6(b)];

$$\Delta\rho_p(\tilde{\ell}) = \frac{\alpha_W}{4\pi}\sum_{i=1}^{2}U_{i1}^2\bigg[\sum_{j,k=1}^{2}\Gamma_{\tau L}^{k3}\Gamma_{\tau L}^{j3}c_{\tau}^{kj}\bigg\{G_0(X_{\tilde{\tau}_j\chi_i^+},X_{\tilde{\tau}_k\chi_i^+}) + \ln\frac{m_{\chi_i^+}^2}{\mu^2}\bigg\} - c_L^{\ell}\bigg\{G_0(X_{\chi_i^+\tilde{\mu}_L},1)+\ln\frac{m_{\tilde{\mu}_L}^2}{\mu^2}\bigg\}\bigg], \tag{16}$$

$$\Delta\rho_p^L(\tilde{\nu}) = \frac{\alpha_W}{4\pi}\sum_{j=1}^{5}G_{\nu L}^{j2}\bigg\{G_0(X_{\chi_j^0\tilde{\nu}_{\tau_L}},1) + \ln\frac{m_{\tilde{\nu}_{\tau_L}}^2}{\mu^2} - (\tilde{\nu}_{\tau_L}\to\tilde{\nu}_{\mu_L})\bigg\}, \tag{17}$$

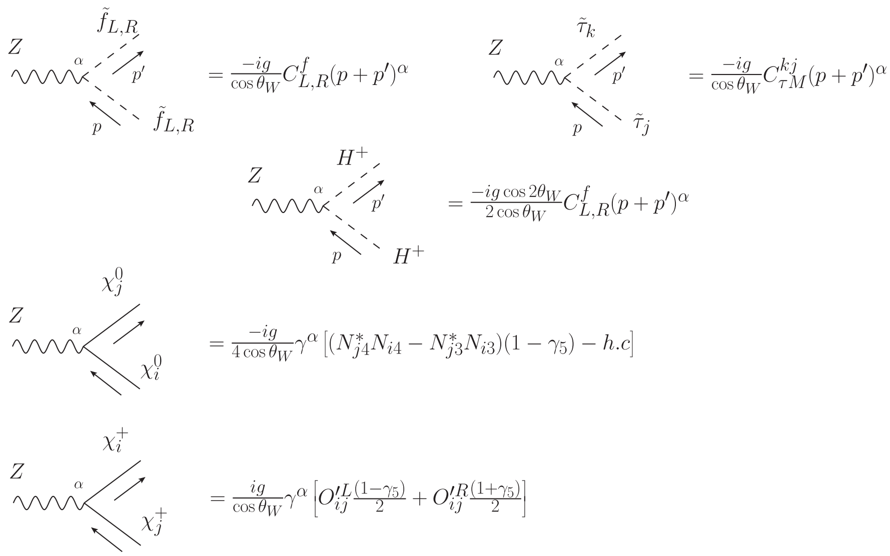

FIG. 4. R-parity conserved vertices with the Z^0 boson.

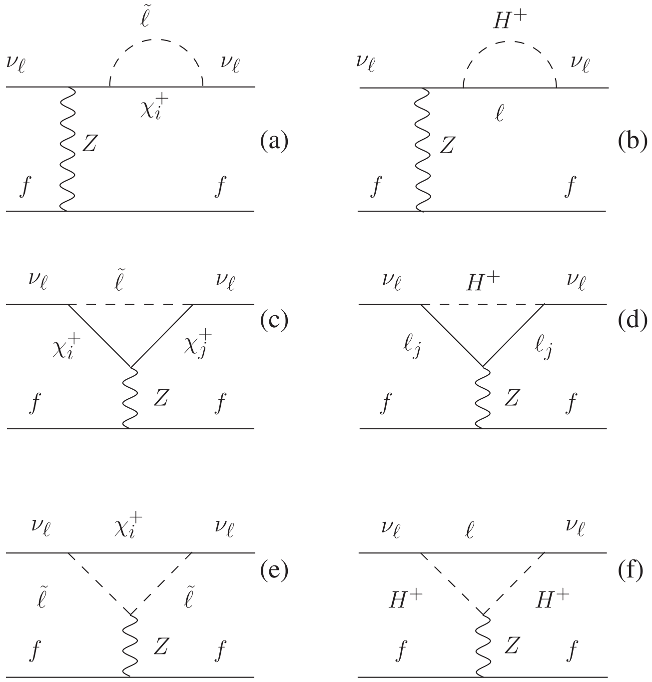

FIG. 5. R-parity conserved penguins and self-energies involving charginos and the charged Higgs.

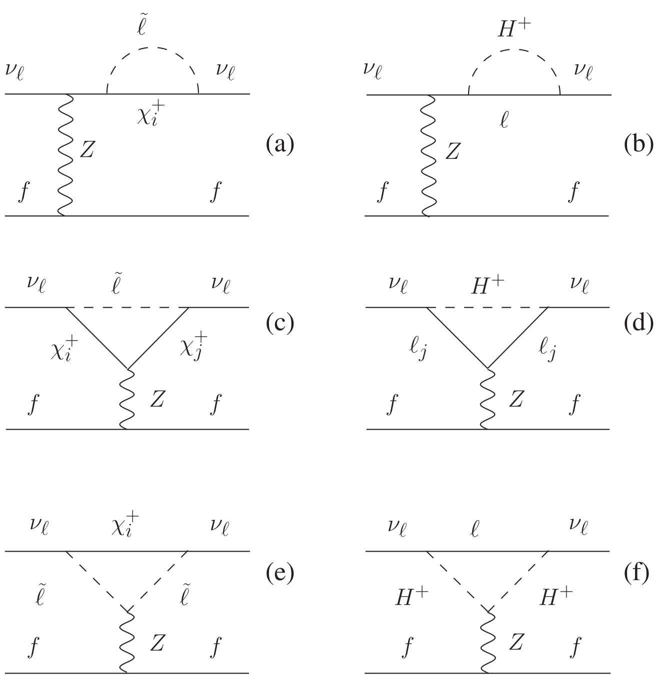

FIG. 6. R-parity conserved penguins and self-energies involving neutralinos.

$$\begin{aligned}\Delta\rho_p(\chi^+) = \frac{\alpha_W}{4\pi}\sum_{i,j=1}^{2} U_{i1}U_{j1} \times \Bigg[\sum_{k=1}^{2}\Gamma_{\tau L}^{k32}\Big\{2\mathcal{O}'^{L}_{ij}H_0(X_{\chi_i^+\tilde{\tau}_k},\\ X_{\chi_j^+\tilde{\tau}_k}) - \mathcal{O}'^{R}_{ij}\Big(G_0(X_{\chi_i^+\tilde{\tau}_k}, X_{\chi_j^+\tilde{\tau}_k}) + \ln\frac{m^2_{\tilde{\tau}_k}}{\mu^2}\Big)\Big\}\\ - \Big\{2\mathcal{O}'^{L}_{ij}H_0(X_{\chi_i^+\tilde{\mu}_L}, X_{\chi_j^+\tilde{\mu}_L})\\ - \mathcal{O}'^{R}_{ij}\Big(G_0(X_{\chi_i^+\tilde{\mu}_L}, X_{\chi_j^+\tilde{\mu}_L}) + \ln\frac{m^2_{\tilde{\mu}_L}}{\mu^2}\Big)\Big\}\Bigg], \quad (18)\end{aligned}$$

$$\begin{aligned}\Delta\rho_p^L(\chi^0) = \frac{\alpha_W}{4\pi}\sum_{i,j=1}^{2} G^i_{\nu L}G^j_{\nu L}\{N_{i4}N_{j4} - N_{i3}N_{j3}\}\\ \times\Big[2H_0(X_{\chi_i^0\tilde{\nu}_{\tau_L}}, X_{\chi_j^0\tilde{\nu}_{\tau_L}}) + \Big\{G_0(X_{\chi_i^0\tilde{\nu}_{\tau_L}}, X_{\chi_j^0\tilde{\nu}_{\tau_L}})\\ + \ln\frac{m^2_{\tilde{\nu}_{\tau_L}}}{\mu^2}\Big\} - (\tilde{\nu}_{\tau_L}\to\tilde{\nu}_{\mu_L})\Big]. \quad (19)\end{aligned}$$

We have neglected the loops involving $\tilde{\mu}_R$.

When we sum all the contributions [Fig. 5(b), 5(d), and 5(f)] involving the charged Higgs boson [9], we find

$$\Delta\rho_p^{H^+} \simeq -\frac{\alpha_W}{4\pi}\frac{m_\tau^2}{M_W^2}\mathrm{tg}^2\beta\frac{y}{2}\Big[\frac{1}{1-y} + \frac{\ln y}{(1-y)^2}\Big].$$

D. Box diagrams

The charge conjugation operators in the vertices of Fig. 2 imply that all box diagrams involving charginos induce radiative corrections to neutrino scattering only, despite the fact that the neutrino fermionic lines of Fig. 7(a) and Fig. 7(b) are oriented on the left. As we did before, we diagonalize the stau mass matrix and we neglect the $\tilde{\mu}_R$ contribution. The box diagrams involving charginos [respectively, Fig. 7(a)–7(c)] are

$$\begin{aligned}\Delta\rho^e_{\mathrm{box}}(\chi^+) = -\frac{\alpha_W}{4\pi}\frac{M_W^2}{m^2_{\tilde{\nu}_e}}\sum_{j,k=1}^{2} V_{j1}V_{k1}U_{j1}U_{k1}\\ \times\Big\{\sum_{i=1}^{2}\Gamma^{i32}_{\tau L}H'(X_{\chi_j^+\tilde{\nu}_e}, X_{\chi_k^+\tilde{\nu}_e}, X_{\tilde{\tau}_i\tilde{\nu}_e})\\ - H'(X_{\chi_j^+\tilde{\nu}_e}, X_{\chi_k^+\tilde{\nu}_e}, X_{\tilde{\mu}_L\tilde{\nu}_e})\Big\}, \quad (20)\end{aligned}$$

$$\Delta\rho^d_{\mathrm{box}}(\chi^+) = \Delta\rho^e_{\mathrm{box}}(\chi^+)(\tilde{\nu}_e\to\tilde{u}_L), \quad (21)$$

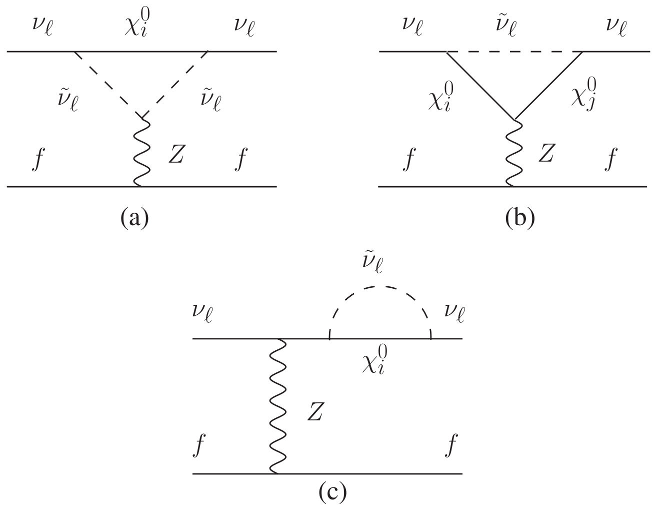

FIG. 7. R-parity conserved box diagrams.

$$\Delta\rho^u_{\rm box}(\chi^+) = -\frac{\alpha_W}{8\pi}\frac{M_W^2}{m^2_{\tilde{d}_L}}\sum_{j,k=1}^{2} U_{j1}^2 U_{k1}^2 \times \Big\{\sum_{i=1}^{2}\Gamma^{i32}_{\tau L} G'(X_{\tilde{\tau}_i\tilde{d}_L}, X_{\chi_j^+\tilde{d}_L}, X_{\chi_k^+\tilde{d}_L}) - G'(X_{\tilde{\mu}_L\tilde{d}_L}, X_{\chi_j^+\tilde{d}_L}, X_{\chi_k^+\tilde{d}_L})\Big\}. \quad (22)$$

The box diagrams involving neutralinos with crossed fermionic lines will only contribute to neurino scattering because the neutrino fermionic lines are oriented on the right. Here, $\tilde{f}_R$ contributions are non-negligible.

We consider here the box diagrams involving neutralinos for neutrino scattering [Fig. 7(d)]:

(i) with left sfermions ($\tilde{e}_L$, $\tilde{u}_L$, $\tilde{d}_L$):

$$\Delta\rho^{\tilde{f}_L}_{\rm box}(\chi^0) = -\frac{\alpha_W}{2\pi}\sum_{j,k=1}^{5} G^k_{\nu L}G^j_{\nu L}G^k_{fL}G^j_{fL}\frac{M_W^2}{m^2_{\tilde{f}_L}} \times [G'(X_{\tilde{\nu}_\tau\tilde{f}_L}, X_{\chi_j^0\tilde{f}_L}, X_{\chi_k^0\tilde{f}_L}) - (\tilde{\nu}_\tau \to \tilde{\nu}_\mu)] \quad (23)$$

(ii) with right sfermions ($\tilde{e}_R$, $\tilde{u}_R$, $\tilde{d}_R$):

$$\Delta\rho^{\tilde{f}_R}_{\rm box}(\chi^0) = \frac{\alpha_W}{\pi}\sum_{j,k=1}^{5} G^k_{\nu L}G^j_{\nu L}G^k_{fR}G^j_{fR}\frac{M_W^2}{m^2_{\tilde{f}_R}} \times [H'(X_{\chi_j^0\tilde{f}_R}, X_{\chi_k^0\tilde{f}_R}, X_{\tilde{\nu}_\tau\tilde{f}_R}) - (\tilde{\nu}_\tau \to \tilde{\nu}_\mu)] \quad (24)$$

Note that the contributions from all box diagrams involving antineutrino scattering are identical to the previous contributions, only the forms of the boxes will be different. For instance if a ladder box was contributing to antineutrinos then the corresponding box for neutrinos will have crossed fermionic lines and vice-versa.

E. Numerical results

The numerical results given just below have been made in the NMSSM framework which is a more efficient supersymmetric model than the MSSM in both theoretical and experimental ways. Indeed, the MSSM is almost ruled out by the experimental constraints (e.g. on the lightest scalar Higgs boson mass) contrary to the NMSSM. Furthermore, since the parameter space is bigger in the NMSSM, we can expect possibly larger values of ε.

We make here a low-energy study where we take first generation sleptons degenerate with the second generation ones, and only allow the third generation sleptons to have a different mass. It is a possibility that sfermion masses may dynamically align along the directions, in flavor space, of the fermion masses, suppressing flavor changing neutral currents but allowing large mass splittings [46].

We consider two experimentally allowed cases for the sleptons with a splitting between the third and the second generation:

(i) $m_{\tilde{\tau}} = 300$ GeV and $m_{\tilde{\mu}} = 200$ GeV (normal supersymmetric hierarchy)

(ii) $m_{\tilde{\tau}} = 200$ GeV and $m_{\tilde{\mu}} = 300$ GeV (inverted supersymmetric hierarchy)

We also assume that squarks are much heavier than sleptons: $M_{\tilde{Q}} = 1$ TeV. These are the effects of gluino masses in the renormalization group evolution of scalar masses.

The splitting among the sleptons of the second and third generations is mainly responsible for the size of $\Delta\rho$.

The purpose of this section is the investigation of the supersymmetric parameter space in some specific cases. To this end we made a subroutine to the Fortran code called NMHDECAY, which is available on the NMSSMTools web page [43,47,48]. This subroutine computes the different R-parity conserved supersymmetric contributions to ε. Note that ε is the same for antineutrinos, as in the standard model.

By making scans over the supersymmetric parameter space, we can obtain, in some regions of the parameter space, divergences for either $m_{\chi_j^+} = m_{\tilde{\tau}_k}$, $m_{\chi_j^+} = m_{\tilde{\mu}_L}$, or $m_{\chi_i^0} = m_{\tilde{\nu}_\ell}$. This is because we assume vanishing external legs.

In supersymmetry, there are many parameters. ε does not depend very much on λ and κ so we fix them as we usually do in supersymmetry: $\lambda = 0.4$ and $\kappa = 0.5$. We allow some other parameters to vary: $\tan\beta$, M_A, and $\mu_{\rm eff}$.

M_A is an effective supersymmetric parameter somewhat equivalent to the second pseudoscalar Higgs mass in our regions of the parameter space.

We show two different illustrative situations motivated by high-energy models for the gaugino masses:

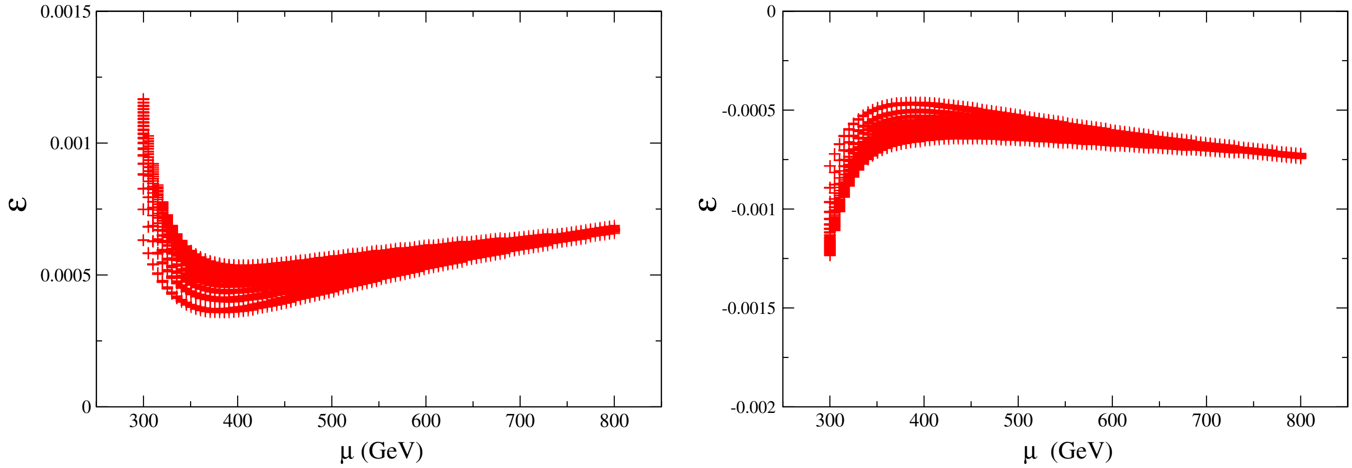

FIG. 8 (color online). ε as a function of μ. We fix $\lambda = 0.4$ and $\kappa = 0.5$. $M_1 = 66$ GeV, $M_2 = 133$ GeV, and $M_3 = 500$ GeV. The figure on the left represents the normal supersymmetric hierarchy ($m_{\tilde{\tau}} = 300$ GeV and $m_{\tilde{\mu}} = 200$ GeV), the figure on the right represents the inverted supersymmetric hierarchy ($m_{\tilde{\tau}} = 200$ GeV and $m_{\tilde{\mu}} = 300$ GeV).

(i) $M_1 = 66$ GeV, $M_2 = 133$ GeV, and $M_3 = 500$ GeV [cf Fig. 8]

(ii) $M_1 = 150$ GeV, $M_2 = 300$ GeV, and $M_3 = 1$ TeV [cf Fig. 9]

In Fig. 8, $\tan\beta$ varies between 2 and 15, M_A varies between 579 and 2000 GeV, μ varies between 300 and 800 GeV. We see in Fig. 8 that contrary to the SM case, $V_{\mu\tau}$ can be either positive or negative.

In Fig. 9, $\tan\beta$ varies between 2 and 18 (for the figure on the left) and between 2 and 9.6 (for the figure on the right), M_A varies between 500 and 1000 GeV, μ varies between 200 and 564 GeV.

On the other hand, as we can see in Fig. 9, ε can go up to 2×10^{-2} in this region of the parameter space. The sign of μ does not have an important impact on the maximal value that ε can reach.

We finally mention that other extensions of the standard model may also lead to sizable effects upon $\Delta n_{\tau\mu}$. In the next section, we will consider supersymmetric R-parity violating interactions which can have important effects on the neutrino indices of refraction already at the tree level [49].

IV. R-PARITY BREAKING SUSY CORRECTIONS

A. Introduction

The superpotential W_{NMSSM} is not the most general superpotential we wan write because there exist some other gauge invariant couplings that we did not take into account. These new couplings break a discrete symmetry called R-parity. This symmetry requires that an interaction must have an even number of SUSY particles. If R-parity is

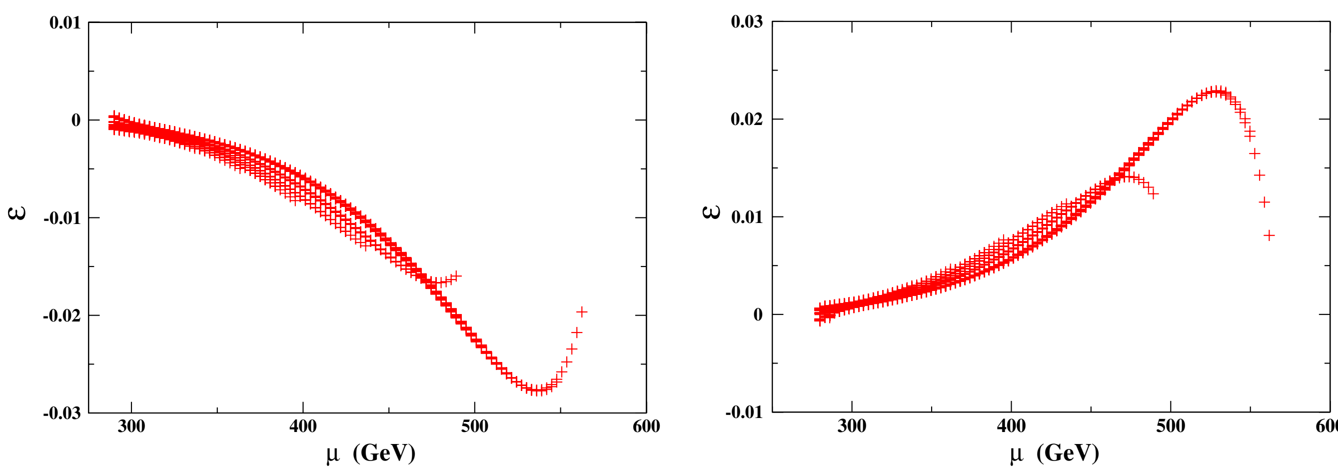

FIG. 9 (color online). ε as a function of μ. We fix $\lambda = 0.4$ and $\kappa = 0.5$. $M_1 = 150$ GeV, $M_2 = 300$ GeV, and $M_3 = 1$ TeV. The figure on the left represents the normal supersymmetric hierarchy, the figure on the right represents the inverted supersymmetric hierarchy.

broken, the LSP will no longer be stable [50]. R-parity violating interactions also violate the lepton number (L) or baryon number (B). To be as general as possible, the superpotential has to contain the following terms [51]:

$$W_{\not R_P} = \sum_{i,j,k} \bigg(\frac{1}{2} \lambda_{ijk} \hat{L}_i \hat{L}_j \hat{E}_k^c + \lambda'_{ijk} \hat{L}_i \hat{Q}_j \hat{D}_k^c + \frac{1}{2} \lambda''_{ijk} \varepsilon_{\alpha\beta\gamma} \hat{U}_i^{c\alpha} \hat{D}_j^{c\beta} \hat{D}_k^{c\gamma} + \mu_i \hat{H}_u \hat{L}_i + \lambda_i \hat{S} \hat{H}_u \hat{L}_i \bigg). \tag{25}$$

The Lagrangian $\mathcal{L}_{\not R_P}$ can be derived using the common procedure [40,52].

If we consider this part of the superpotential:

$$W_{\text{masses}} = W_{\text{NMSSM}} + \mu_i \hat{H}_u \hat{L}_i + \lambda_i \hat{S} \hat{H}_u \hat{L}_i, \tag{26}$$

we can generate two neutrino masses at the tree level [40] by mixing neutrinos and neutralinos. By considering a seesaw-like mechanism, the mass matrix is

$$\mathcal{M}_{\tilde{\chi}^0} = \begin{pmatrix} \mathcal{M}_{\text{NMSSM}} & \xi_{\not R_P}^T \\ \xi_{\not R_P} & 0_{3\times 3} \end{pmatrix}, \tag{27}$$

where $\mathcal{M}_{\text{NMSSM}}$ is the R-parity conserved neutralino mass matrix and $\xi_{\not R_P}$ is the part of the mass matrix induced by R-parity violation which mix neutralinos and neutrinos. We will assume here: $v_i/v_{u,d} \ll 1$, $|\mu_i/\mu| \ll 1$, and $|\lambda_i/\lambda| \ll 1$ in order to reproduce the neutrino phenomenology. v_i are the v.e.v. of the sneutrinos. This model is self-consistent because we give here a way to generate the neutrino masses contrary to many other scenarios of radiative corrections on neutrino indices of refraction.

In the following, $\nu_i = N_{ij} \tilde{\Psi}_j$ where $\tilde{\Psi}^T = (\tilde{B}, \tilde{W}_3, \tilde{h}_u, \tilde{h}_d, \tilde{s}, \nu_e, \nu_\mu, \nu_\tau)$, $i = 1 \dots 3$ and $j = 1 \dots 8$. ν_e, ν_μ and ν_τ represent the neutrinos in their flavour basis, ν_i represent the neutrinos in their mass basis. $\chi_i^0 = N_{(i+3)j} \tilde{\Psi}_j$ where $i = 1 \dots 5$ and $j = 1 \dots 8$. χ_i^0 are the five NMSSM's neutralinos.

Note that neutrino masses can be generated at the tree level in different models such as models with seesaw mechanisms [53,54] even in the limit of massless neutrinos. However, we have chosen here to work in the NMSSM framework with R-parity breaking. Some specific models allow us to generate neutrino masses with R-parity breaking, the most popular one is the pure bilinear model (with only $\mu_i \hat{H}_u \hat{L}_i$) in the MSSM. In this model, only one neutrino mass is generated at the tree level [55]. In our model, we consider all R-parity breaking terms in the NMSSM and two neutrino masses are generated.

B. Tree-level corrections

Because of R-parity breaking, new interactions are possible between SUSY particles. This yields new one-loop corrections but also tree-level corrections contrary to the R-parity conserved case. Such tree-level corrections in the supernova context have been partially studied in [49,56]. Since this work focuses on $V_{\mu\tau}$, we only concentrate on graphs involving μ and τ neutrinos. Moreover, we only consider neutrinos which do not change flavor after the R-parity breaking interaction, therefore, we are not concerned by an off-diagonal term in the matter Hamiltonian.

Here, we give a specific contribution to antineutrino scattering [Fig. 10(a)] with left sleptons $\tilde{\ell}_{L,i}$:

$$\Delta\rho_a(\tilde{\ell}_{L,i}) = -\sum_{i=1}^{3} \frac{(\lambda_{3i1}^2 - \lambda_{2i1}^2)}{g^2} \frac{M_W^2}{m_{\tilde{\ell}_{L,i}}^2}. \tag{28}$$

With left down squarks $\tilde{d}_{L,i}$ [Fig. 10(b)],

$$\Delta\rho_b(\tilde{d}_{L,i}) = \Delta\rho_a(\tilde{\ell}_{L,i})(\lambda_{ki1} \to \lambda'_{ki1}, \tilde{\ell}_{L,i} \to \tilde{d}_{L,i}). \tag{29}$$

The right sleptons $\tilde{\ell}_{R,i}$ and the right down squarks $\tilde{d}_{R,i}$ do not contribute.

The following contributions induce corrections to both neutrino and antineutrino scattering: for the diagram of Fig. 10(c):

$$\Delta\rho_c(\chi^0) = -\sum_{j,k=1}^{5} (N_{(j+3)8} N_{(i+3)8} - N_{(j+3)7} N_{(i+3)7}) \times (N_{(j+3)4} N_{(i+3)4} - N_{(j+3)3} N_{(i+3)3}), \tag{30}$$

for the diagram of Fig. 10(d):

$$\Delta\rho_d(\tilde{\ell}_{L,i}) = \Delta\rho_a(\tilde{\ell}_{L,i}), \tag{31}$$

for the diagram of Fig. 10(e):

$$\Delta\rho_e(\tilde{d}_{L,i}) = \Delta\rho_b(\tilde{d}_{L,i}). \tag{32}$$

For Fig. 10(d) and 10(e), the right sleptons $\tilde{\ell}_{R,i}$ and the right down squarks $\tilde{d}_{R,i}$ do not contribute. Let us now

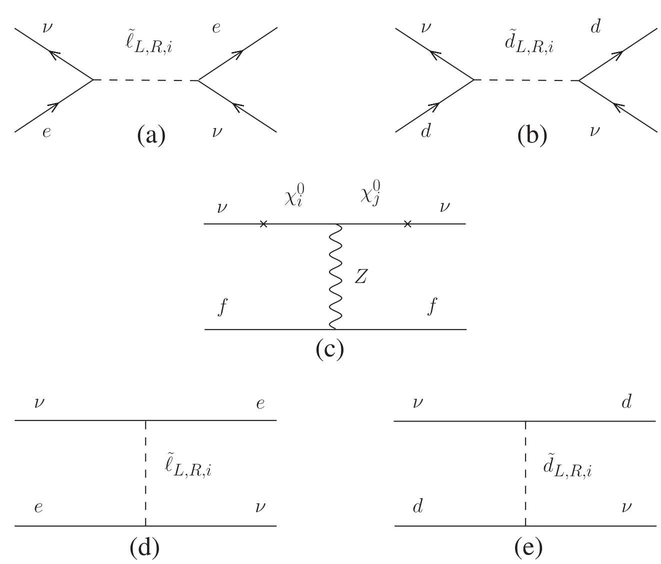

FIG. 10. R-parity broken tree-level corrections.

discuss in the relevant cases the values of the R-parity breaking contributions. In general, except for values of supersymmetric masses which imply divergences in the vanishing external legs approximation for the loop functions defined above, the tree-level contributions will dominate all the one-loop R-parity breaking contributions.

As seen in the previous subsection, the R-parity breaking interactions are controlled by some parameters: μ_i, λ_i, λ_{ijk}, λ'_{ijk}, and λ''_{ijk}. The two former ones allow us to generate two neutrino masses at the tree level, hence they are constrained by the values of Δm^2_{12} and Δm^2_{23}: typically $|\mu_i| \sim 10^{-6}|\mu_{\rm eff}|$ and $|\lambda_i| \sim 10^{-6}|\lambda|$. This implies that $|N_{(j+3)6}|, |N_{(j+3)7}|, |N_{(j+3)8}| = O(10^{-6})$.

Concerning the parameters λ_{ijk}, λ'_{ijk}, and λ''_{ijk}, apart from a few isolated cases, the bounds derived under the so-called single coupling dominance hypothesis, (where a single $\not{R}_P$ coupling is assumed to dominate over all the others) are in general moderately strong. The typical orders of magnitude of such couplings, which can be $|\lambda_{ijk}|$ or $|\lambda'_{ijk}|$ or $|\lambda''_{ijk}|$, are $<10^{-2} - 10^{-1}$ [57]. Note that the constraints on these parameters are independent of the μ_i and λ_i constraints.

For instance, if we assume that the only nonvanishing parameters are λ''_{ijk}, we can see from the previous sections that the $\not{R}_P$ contributions for the tree-level order will be reduced to the contribution of Eq. (30).

Nevertheless, if the nonvanishing parameters are λ_{ijk} or λ'_{ijk}, the $\not{R}_P$ contributions will possibly be of the same order of magnitude or even bigger than the R-parity conserved contributions. For example, if we assume λ_{ijk} to be dominant and of the order $O(10^{-1})$, the contributions of Eqs. (29), (30), and (32) will vanish whereas the contributions of Eqs. (28) and (31) to ε will be of the order $O(10^{-3})$. If we compare these values to the ones of Fig. 8, we can verify that the $\not{R}_P$ contributions can be bigger than the R-parity conserved contributions.

On the other hand, if we do not make an hypothesis on the values of λ_{ijk}, λ'_{ijk}, and λ''_{ijk}, one can see that the strongest constraints on these parameters come from the single nucleon decay [52,57]: $|\lambda_{ijk}\lambda''_{lmn}| < [O(10^{-12}) - O(10^{-3})]$ and $|\lambda'_{ijk}\lambda''_{lmn}| < O(10^{-9})$. If we assume the parameters λ_{ijk}, λ'_{ijk}, and λ''_{ijk} to be of the same order of magnitude, apart from very specific cases, the $\not{R}_P$ contributions will always be negligible.

Note that very strong constraints may come from cosmological and astrophysical bounds but they are very sensitive on the LSP chosen (like neutralino, sneutrino, gravitino,...) [50] and on the model.

C. Self-energy corrections

We willingly leave certain factors not simplified to be able to compare with other corrections more rapidly. All the contributions will be equal for neutrino and antineutrino scattering.

For Fig. 11(a):

$$\Delta\rho^{\tilde{\ell}_R}(\Sigma) = -\frac{\alpha_W}{8\pi}\sum_{i,j=1}^{3}\frac{(\lambda^2_{3ij}-\lambda^2_{2ij})}{g^2} \times\left\{G_0(X_{\ell_i\tilde{\ell}_{R,j}},1)+\ln\frac{m^2_{\tilde{\ell}_{R,j}}}{\mu^2}\right\},$$
$$\Delta\rho^{\tilde{d}_R}(\Sigma) = \Delta\rho^{\tilde{\ell}_R}(\Sigma)(\lambda_{kij}\to\lambda'_{kij},\tilde{\ell}_{R,j}\to\tilde{d}_{R,j}). \qquad (33)$$

For Fig. 11(c):

$$\Delta\rho^{\tilde{\ell}_L}(\Sigma) = \Delta\rho^{\tilde{\ell}_R}(\Sigma)(\lambda_{kij}\to\lambda_{kji},\tilde{\ell}_{R,j}\to\tilde{\ell}_{L,j}),$$
$$\Delta\rho^{\tilde{d}_L}(\Sigma) = \Delta\rho^{\tilde{\ell}_R}(\Sigma)(\lambda_{kij}\to\lambda'_{kji},\tilde{\ell}_{R,j}\to\tilde{d}_{L,j}). \qquad (34)$$

In the R-parity breaking scenario, there are NMSSM specific self-energies due to the term $\lambda_i\hat{S}\hat{H}_u\hat{L}_i$ in the superpotential. This term induced one new coupling between a neutrino, one Higgs (scalar or pseudoscalar), and a neutralino. We present here the contributions for scalar Higgses and for pseudoscalar Higgses.

For both Fig. 11(b) and 11(d), the contribution from scalar Higgses:

$$\Delta\rho^{h}(\Sigma) = -\frac{\alpha_W}{8\pi}\frac{(\lambda_3^2-\lambda_2^2)}{g^2}\sum_{i=1}^{5}\sum_{j=1}^{3}(N^2_{(i+3)5}S^2_{j1} + N^2_{(i+3)3}S^2_{j3})\left\{G_0(X_{\chi_i^0 h_j},1)+\ln\frac{m^2_{h_j}}{\mu^2}\right\}; \qquad (35)$$

from pseudoscalar Higgses:

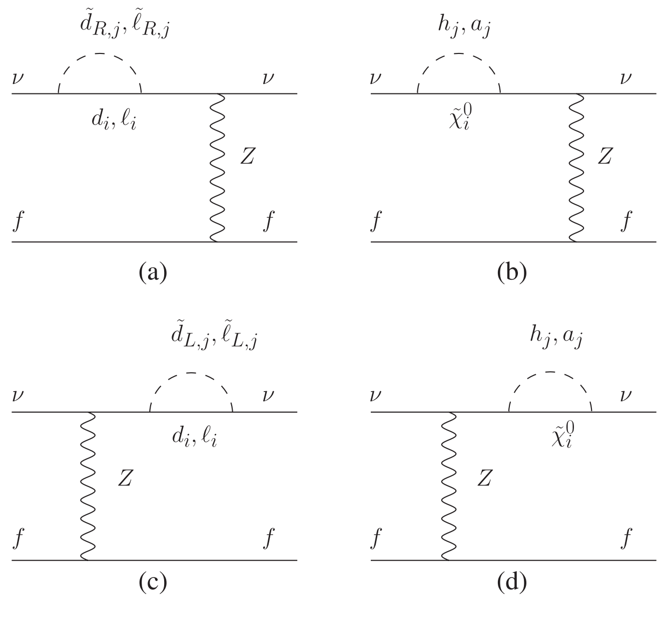

FIG. 11. R-parity broken self-energy corrections.

$$\Delta\rho^a(\Sigma) = -\frac{\alpha_W}{8\pi}\frac{(\lambda_3^2-\lambda_2^2)}{g^2}\sum_{i=1}^{5}\sum_{j=1}^{2}(N^2_{(i+3)5}P^2_{j1} + N^2_{(i+3)3}P^2_{j3})\left\{G_0(X_{\chi_i^0 a_j},1) + \ln\frac{m^2_{a_j}}{\mu^2}\right\}. \quad (36)$$

Note that the self-energy contributions will always be negligible with respect to the tree-level ones except for $m^2_{\chi_i^0} = m^2_{h_j}$ or $m^2_{\chi_i^0} = m^2_{a_j}$ which may induce important values for NMSSM specific contributions of Eqs. (35) and (36), especially in the case where the only nonvanishing parameters are λ''_{ijk}.

D. Penguin type diagrams

We consider here the penguin diagrams. All the contributions will be equal for neutrino and antineutrino scattering.

For the diagram of Fig. 12(a) and 12(c):

$$\Delta\rho_P^{\tilde{\ell}_L}(\ell) = -\frac{\alpha_W}{16\pi}\sum_{i,j=1}^{3}\frac{(\lambda^2_{3ji}-\lambda^2_{2ji})}{g^2}\times\left[G_0(X_{\tilde{\ell}_{L,j},\ell_i},1) + \ln\left(\frac{m^2_{\ell_i}}{\mu^2}\right)\right],$$
$$\Delta\rho_P^{\tilde{d}_L}(d) = \Delta\rho_P^{\tilde{\ell}_L}(\ell)(\lambda_{kji}\to\lambda'_{kji}, \tilde{\ell}_{L,j}\to\tilde{d}_{L,j}, \ell_i\to d_i). \quad (37)$$

For the diagram of Fig. 12(b) and 12(d):

$$\Delta\rho_P^{\ell}(\tilde{\ell}_L) = -\frac{\alpha_W}{4\pi}c_L^{\ell}\sum_{i,j=1}^{3}\frac{(\lambda^2_{3ji}-\lambda^2_{2ji})}{g^2}\times\left[G_0(X_{\ell_i,\tilde{\ell}_{L,j}},1) + \ln\left(\frac{m^2_{\tilde{\ell}_{L,j}}}{\mu^2}\right)\right],$$
$$\Delta\rho_P^{d}(\tilde{d}_L) = \Delta\rho_P^{\ell}(\tilde{\ell}_L)(\lambda_{kji}\to\lambda'_{kji}, \tilde{\ell}_{L,j}\to\tilde{d}_{L,j}, \ell_i\to d_i). \quad (38)$$

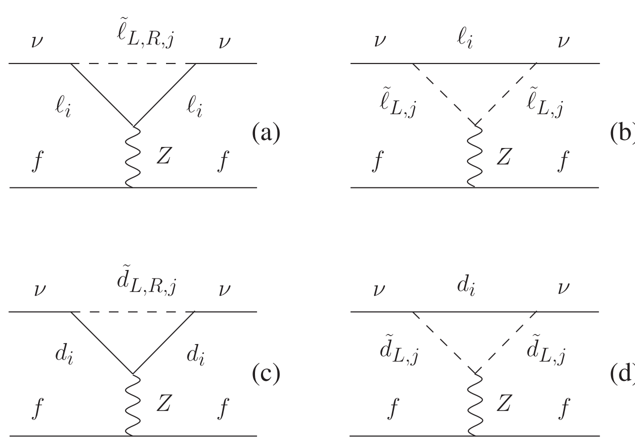

FIG. 12. R-parity broken penguin-type diagrams.

For all the previous penguin diagrams, the right sleptons $\tilde{\ell}_{R,j}$ and the right squarks $\tilde{d}_{R,j}$ do not contribute.

We have below NMSSM specific penguins also due to the term $\lambda_i\hat{S}\hat{H}_u\hat{L}_i$ in the superpotential.

For the diagram of Fig. 13(c):

$$\Delta\rho_P^h(\chi^0) = -\frac{\alpha_W}{8\pi}\frac{\lambda_3^2-\lambda_2^2}{g^2}\sum_{i,j=1}^{5}\sum_{m=1}^{3}N_{(i+3)5}N_{(j+3)5}S^2_{m1}\times(N_{(j+3)4}N_{(i+3)4} - N_{(j+3)3}N_{(i+3)3})\times\left[2H_0(X_{\chi_i^0 h_m}, X_{\chi_j^0 h_m}) + \left\{G_0(X_{\chi_i^0 h_m}, X_{\chi_j^0 h_m}) + \ln\frac{m^2_{h_m}}{\mu^2}\right\}\right]. \quad (39)$$

For the diagram of Fig. 13(a):

$$\Delta\rho_P^a(\chi^0) = -\frac{\alpha_W}{8\pi}\frac{\lambda_3^2-\lambda_2^2}{g^2}\sum_{i,j=1}^{5}\sum_{n=1}^{2}N_{(i+3)5}N_{(j+3)5}P^2_{n1}\times(N_{(j+3)4}N_{(i+3)4} - N_{(j+3)3}N_{(i+3)3})\times\left[2H_0(X_{\chi_i^0 a_n}, X_{\chi_j^0 a_n}) + \left\{G_0(X_{\chi_i^0 a_n}, X_{\chi_j^0 a_n}) + \ln\frac{m^2_{a_n}}{\mu^2}\right\}\right]. \quad (40)$$

We have two identical contributions from the diagram of Fig. 13(b) and 13(d) and we obtain

$$\Delta\rho_P^{\chi^0} = -\frac{\alpha_W}{4\pi}\frac{\lambda_3^2-\lambda_2^2}{g^2}\sum_{i=1}^{5}\sum_{m=1}^{3}\sum_{n=1}^{2}N^2_{(i+3)5}S_{m1}P_{n1}A_M^{mn}\times\left\{G_0(X_{h_m\chi_i^0}, X_{a_n\chi_i^0}) + \ln\frac{m^2_{\chi_i^0}}{\mu^2}\right\}, \quad (41)$$

where $A_M^{mn} = S_{m1}P_{n1} - S_{m2}P_{n2}$ following the notation of [43].

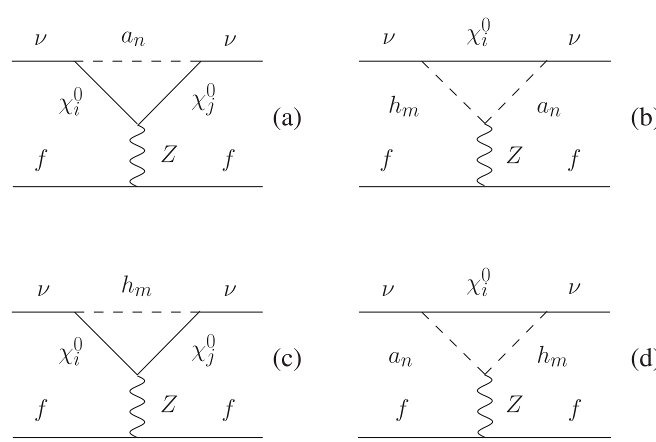

FIG. 13. R-parity broken NMSSM specific penguin-type diagrams.

Note that the penguin contributions will always be negligible with respect to the tree-level ones except for $m^2_{\chi^0_i} = m^2_{h_j}$ or $m^2_{\chi^0_i} = m^2_{a_j}$ which may induce important values for NMSSM specific contributions of Eqs. (39)–(41), especially in the case where the only nonvanishing parameters are λ''_{ijk}.

E. Box diagrams

1. R-parity broken box diagrams

We present in this section the box diagrams' corrections. Each box diagram correction involves Fierz transformations to obtain a similar form as the standard model tree-level interaction. The box diagrams with crossed fermions lines [Fig. 14(b), 14(d), 14(f), 14(h), 14(j), and 14(l)] will only contribute to neurinos, meanwhile the uncrossed fermion lines [Fig. 14(a), 14(c), 14(e), 14(g), 14(i), and 14(k)] will contribute to antineutrinos. However, the contributions to antineutrino scattering will be exactly the same as the contributions to neutrino scattering. We show below the contributions to neutrino scattering.

For the diagram of Fig. 14(j) with $\tilde{\ell}_{L,i} - \tilde{d}_{R,m}$:

$$\Delta\rho^{\nu 2}_{\rm box}(\tilde{\ell}_L - \tilde{d}_R) = -\frac{\alpha_W}{8\pi}\sum_{i,j,k,m=1}^{3}\frac{M_W^2}{m^2_{\tilde{d}_{R,m}}} \times \frac{(\lambda_{3ij}\lambda_{3ik} - \lambda_{2ij}\lambda_{2ik})\lambda'_{j1m}\lambda'_{k1m}}{g^4} \times G'(X_{\ell_j,\tilde{d}_{R,m}}, X_{\ell_k,\tilde{d}_{R,m}}, X_{\tilde{\ell}_{L,i},\tilde{d}_{R,m}}). \quad (42)$$

For the diagram of Fig. 14(d) with $\tilde{d}_{L,i} - \tilde{\ell}_{L,m}$ and the diagram of Fig. 14(f) with $\tilde{d}_{L,i} - \tilde{u}_{L,m}$:

$$\Delta\rho^{r2}_{\rm box}(\tilde{d}_L - \tilde{\ell}_L) = \Delta\rho^{\nu 2}_{\rm box}(\tilde{\ell}_L - \tilde{d}_R)(\lambda \to \lambda', \lambda'_{j1m}\lambda'_{k1m} \to \lambda'_{m1j}\lambda'_{m1k}, \ell_{j,k} \to d_{j,k}, \tilde{\ell}_{L,i} \to \tilde{d}_{L,i}, \tilde{d}_{R,m} \to \tilde{\ell}_{L,m}),$$
$$\Delta\rho^{s2}_{\rm box}(\tilde{d}_L - \tilde{u}_L) = \Delta\rho^{r2}_{\rm box}(\tilde{d}_L - \tilde{\ell}_L)(\lambda'_{m1j}\lambda'_{m1k} \to \lambda'_{1mj}\lambda'_{1mk}, \tilde{\ell}_{L,m} \to \tilde{u}_{L,m}). \quad (43)$$

For the diagram of Fig. 14(d) with $\tilde{d}_{R,i} - \tilde{\ell}_{L,m}$ and the diagram of Fig. 14(f) with $\tilde{d}_{R,i} - \tilde{u}_{L,m}$:

$$\Delta\rho^{r2}_{\rm box}(\tilde{d}_R - \tilde{\ell}_L) = \frac{\alpha_W}{4\pi}\sum_{i,j,k,m=1}^{3}\frac{M_W^2}{m^2_{\tilde{\ell}_{L,m}}} \times \frac{(\lambda'_{3ji}\lambda'_{3ki} - \lambda'_{2ji}\lambda'_{2ki})\lambda'_{m1j}\lambda'_{m1k}}{g^4} \times H'(X_{d_j,\tilde{\ell}_{L,m}}, X_{d_k,\tilde{\ell}_{L,m}}, X_{\tilde{d}_{R,i},\tilde{\ell}_{L,m}}),$$
$$\Delta\rho^{s2}_{\rm box}(\tilde{d}_R - \tilde{u}_L) = \Delta\rho^{r2}_{\rm box}(\tilde{d}_R - \tilde{\ell}_L)(\lambda'_{m1j}\lambda'_{m1k} \to \lambda'_{1mj}\lambda'_{1mk}, \tilde{\ell}_{L,m} \to \tilde{u}_{L,m}). \quad (44)$$

For the diagram of Fig. 14(b) with $\tilde{d}_{R,i} - \tilde{\nu}_{L,m}$ and for the diagram of Fig. 14(h) with $\tilde{\ell}_{R,i} - \tilde{\nu}_{L,m}$:

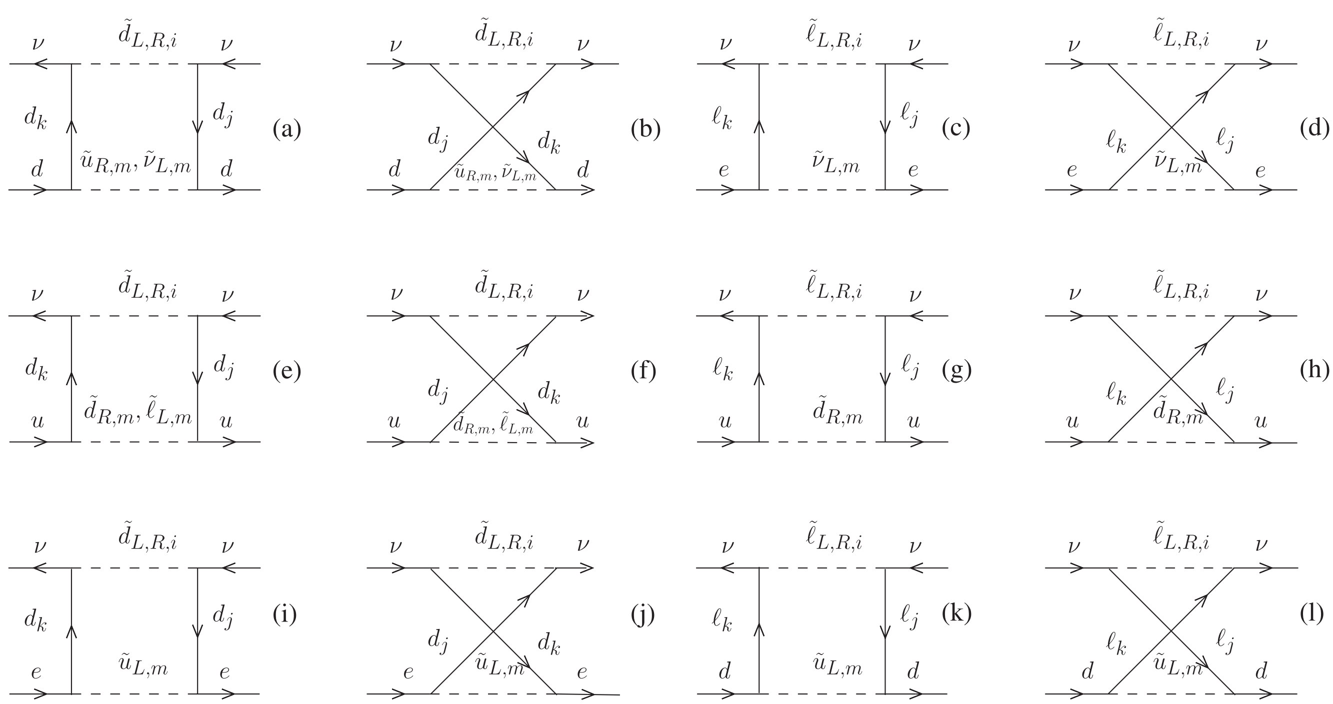

FIG. 14. R-parity broken box diagrams.

$$\Delta\rho^{q2}_{\rm box}(\tilde{d}_R - \tilde{\nu}_L) = \frac{\alpha_W}{4\pi}\sum_{i,j,k,m=1}^{3}\frac{M_W^2}{m^2_{\tilde{\nu}_{L,m}}} \times \frac{(\lambda'_{3ij}\lambda'_{3ik} - \lambda'_{2ij}\lambda'_{2ik})\lambda'_{mj1}\lambda'_{mk1}}{g^4} \times H'(X_{d_j,\tilde{\nu}_{L,m}}, X_{d_k,\tilde{\nu}_{L,m}}, X_{\tilde{d}_{R,i},\tilde{\nu}_{L,m}}),$$

$$\Delta\rho^{u2}_{\rm box}(\tilde{\ell}_R - \tilde{\nu}_L) = \Delta\rho^{q2}_{\rm box}(\tilde{d}_R - \tilde{\nu}_L)(\lambda'_{mj1}\lambda'_{mk1} \to \lambda'_{m1j}\lambda'_{m1k} \text{ then } \lambda' \to \lambda,\, d_{j,k} \to \ell_{j,k},\, \tilde{d}_{R,i} \to \tilde{\ell}_{R,i}). \quad (45)$$

For the diagram of Fig. 14(j) with $\tilde{\ell}_{R,i} - \tilde{d}_{R,m}$ and for the diagram of Fig. 14(l) with $\tilde{\ell}_{L,i} - \tilde{u}_{L,m}$:

$$\Delta\rho^{v2}_{\rm box}(\tilde{\ell}_R - \tilde{d}_R) = \frac{\alpha_W}{4\pi}\sum_{i,j,k,m=1}^{3}\frac{M_W^2}{m^2_{\tilde{d}_{R,m}}} \times \frac{(\lambda_{3ji}\lambda_{3ki} - \lambda_{2ji}\lambda_{2ki})\lambda'_{j1m}\lambda'_{k1m}}{g^4} \times H'(X_{\ell_j,\tilde{d}_{R,m}}, X_{\ell_k,\tilde{d}_{R,m}}, X_{\tilde{\ell}_{R,i},\tilde{d}_{R,m}}),$$

$$\Delta\rho^{w2}_{\rm box}(\tilde{\ell}_L - \tilde{u}_L) = \Delta\rho^{v2}_{\rm box}(\tilde{\ell}_R - \tilde{d}_R)(\lambda'_{j1m}\lambda'_{k1m} \to \lambda'_{jm1}\lambda'_{km1},\, \tilde{d}_{R,m} \to \tilde{u}_{L,m},\, \tilde{\ell}_{R,i} \to \tilde{\ell}_{L,i}). \quad (46)$$

For the diagram of Fig. 14(d) with $\tilde{d}_{L,i} - \tilde{d}_{R,m}$:

$$\Delta\rho^{r2}_{{\rm box},\alpha\sigma}(\tilde{d}_L - \tilde{d}_R) = \frac{\alpha_W}{4\pi}\sum_{i,j,k,m=1}^{3}\sum_{\beta,\delta,\gamma=1}^{3}\frac{M_W^2}{m^2_{\tilde{d}^\gamma_{R,m}}} \times \frac{(\lambda'_{3ij}\lambda'_{3ik} - \lambda'_{2ij}\lambda'_{2ik})\lambda''_{1mj}\lambda''_{1mk}}{g^4} \times \epsilon_{\sigma\gamma\delta}\epsilon_{\alpha\gamma\beta}H'(X_{d^\delta_j,\tilde{d}^\gamma_{R,m}}, X_{d^\beta_k,\tilde{d}^\gamma_{R,m}}, X_{\tilde{d}_{L,i},\tilde{d}^\gamma_{R,m}}). \quad (47)$$

For the diagram of Fig. 14(b) with $\tilde{d}_{R,i} - \tilde{u}_{R,m}$:

$$\Delta\rho^{q2}_{{\rm box},\beta\sigma}(\tilde{d}_R - \tilde{u}_R) = \frac{\alpha_W}{16\pi}\sum_{i,j,k,m=1}^{3}\sum_{\alpha,\delta,\gamma=1}^{3}\frac{M_W^2}{m^2_{\tilde{u}^\alpha_{R,m}}} \times \frac{(\lambda'_{3ji}\lambda'_{3ki} - \lambda'_{2ji}\lambda'_{2ki})\lambda''_{mj1}\lambda''_{mk1}}{g^4} \times \epsilon_{\alpha\delta\sigma}\epsilon_{\alpha\gamma\beta}H'(X_{d^\gamma_j,\tilde{u}^\alpha_{R,m}}, X_{d^\delta_k,\tilde{u}^\alpha_{R,m}}, X_{\tilde{d}_{R,i},\tilde{u}^\alpha_{R,m}}). \quad (48)$$

The indices of ϵ denote $SU(3)$ color indices where ϵ is antisymmetric, $\epsilon_{\alpha\beta\gamma} = \epsilon_{\beta\gamma\alpha} = \epsilon_{\gamma\alpha\beta}$. For example, for the diagram of Fig. 14(b) with $\tilde{d}_{L,i} - \tilde{u}_{R,m}$, the down quark on the left carries the index β and the down quark on the right carries the index σ:

$$\Delta\rho^{q2}_{{\rm box},\beta\sigma}(\tilde{d}_L - \tilde{u}_R) = \frac{\alpha_W}{16\pi}\sum_{i,j,k,m=1}^{3}\sum_{\alpha,\delta,\gamma=1}^{3}\frac{M_W^2}{m^2_{\tilde{u}^\alpha_{R,m}}}\frac{(\lambda'_{3ij}\lambda'_{3ik} - \lambda'_{2ij}\lambda'_{2ik})\lambda''_{m1j}\lambda''_{m1k}}{g^4} \times \epsilon_{\alpha\sigma\delta}\epsilon_{\alpha\beta\gamma}\left[H'(X_{d^\delta_j,\tilde{u}^\alpha_{R,m}}, X_{d^\gamma_k,\tilde{u}^\alpha_{R,m}}, X_{\tilde{d}_{L,i},\tilde{u}^\alpha_{R,m}}) - \frac{G'(X_{d^\delta_j,\tilde{u}^\alpha_{R,m}}, X_{d^\gamma_k,\tilde{u}^\alpha_{R,m}}, X_{\tilde{d}_{L,i},\tilde{u}^\alpha_{R,m}})}{2}\right]. \quad (49)$$

The diagram of Fig. 14(b) with $\tilde{d}_{L,i} - \tilde{\nu}_{L,m}$ can be deducted from the previous one by removing the ϵ factors and by taking a factor 4 and $\lambda'' \to \lambda'$, $\tilde{u}_R \to \tilde{\nu}_L$:

$$\Delta\rho^{q2}_{\rm box}(\tilde{d}_L - \tilde{\nu}_L) = \frac{\alpha_W}{4\pi}\sum_{i,j,k,m=1}^{3}\frac{M_W^2}{m^2_{\tilde{\nu}_{L,m}}}\frac{(\lambda'_{3ij}\lambda'_{3ik} - \lambda'_{2ij}\lambda'_{2ik})\lambda'_{mj1}\lambda'_{mk1}}{g^4} \times \left[H'(X_{d_j,\tilde{\nu}_{L,m}}, X_{d_k,\tilde{\nu}_{L,m}}, X_{\tilde{d}_{L,i},\tilde{\nu}_{L,m}}) - \frac{G'(X_{d_j,\tilde{\nu}_{L,m}}, X_{d_k,\tilde{\nu}_{L,m}}, X_{\tilde{d}_{L,i},\tilde{\nu}_{L,m}})}{2}\right]. \quad (50)$$

Finally, for the diagram of Fig. 14(h) with $\tilde{\ell}_{L,i} - \tilde{\nu}_{L,m}$:

$$\Delta\rho^{u2}_{\rm box}(\tilde{\ell}_L - \tilde{\nu}_L) = \Delta\rho^{q2}_{\rm box}(\tilde{d}_L - \tilde{\nu}_L)(\lambda' \to \lambda,\, d_{j,k} \to \ell_{j,k},\, \tilde{d}_{L,i} \to \tilde{\ell}_{L,i}). \quad (51)$$

The rest of diagrams do not contribute because of a different form as the correct tree-level standard model form given in Eq. (3).

In general, the box contributions will be negligible with respect to the tree-level ones. However, if we assume the single coupling dominance hypothesis, we will have to consider three cases:

(a) The only nonvanishing parameters are λ_{ijk}: if $m^2_{\tilde{\ell}_{R,i}} = m^2_{\tilde{\nu}_{L,m}}$ or $m^2_{\tilde{\ell}_{L,i}} = m^2_{\tilde{\nu}_{L,m}}$, the contributions $\Delta\rho^{u2}_{\rm box}(\tilde{\ell}_R - \tilde{\nu}_L)$ or $\Delta\rho^{u2}_{\rm box}(\tilde{\ell}_L - \tilde{\nu}_L)$ can become important.

(b) The only nonvanishing parameters are λ'_{ijk}: if $m^2_{\tilde{d}_{L,i}} = m^2_{\tilde{u}_{L,m}}$ or $m^2_{\tilde{d}_{R,i}} = m^2_{\tilde{u}_{L,m}}$, the contributions $\Delta\rho^{s2}_{\rm box}(\tilde{d}_L - \tilde{u}_L)$ or $\Delta\rho^{s2}_{\rm box}(\tilde{d}_R - \tilde{u}_L)$ can become important.

(c) The only nonvanishing parameters are λ''_{ijk}: all the box contributions vanish.

2. Cancelling diagrams

It is interesting to notice that amongst the possible radiative corrections induced by the R-parity breaking interactions, some of them cancel. Contrary to the previous box diagrams, all box diagrams in Fig. 15 should contribute equally to neutrinos and antineutrinos because the fermionic lines do not link the neutrinos to the fermion

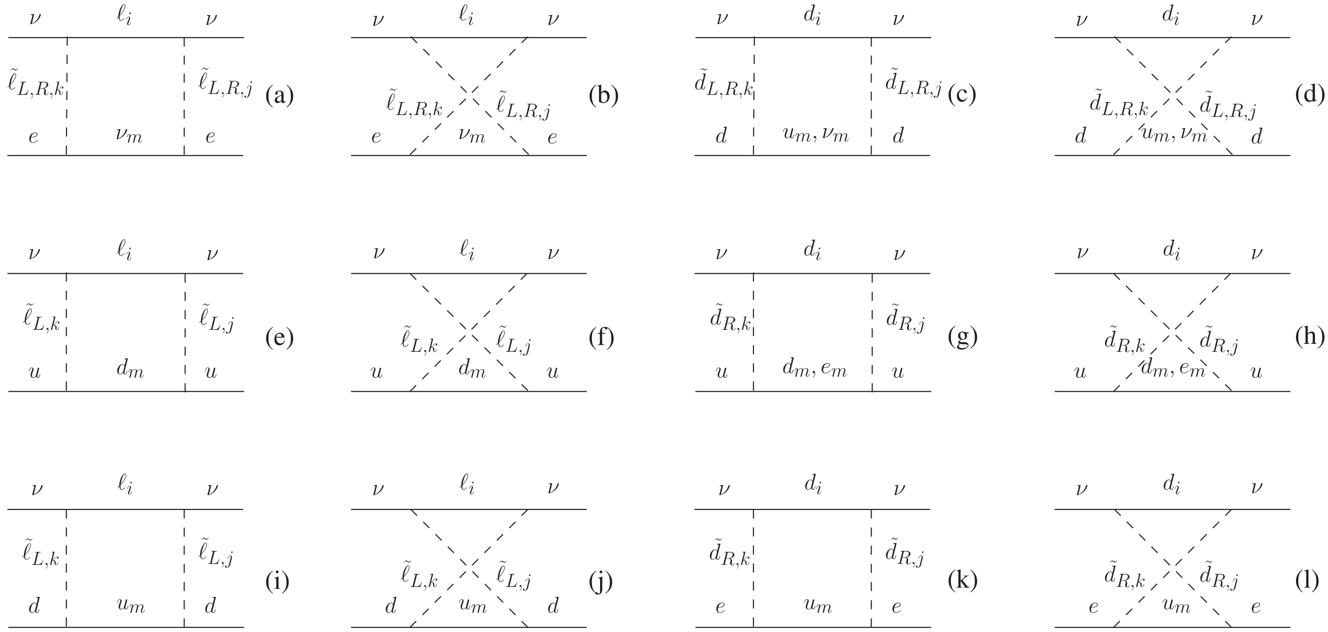

FIG. 15. R-parity broken radiative corrections which cancel out. The Feynman graphs with uncrossed scalar lines on the left cancel with the Feynman graphs with crossed scalar lines on the right.

present in the external leg. The particles exchanged between the two fermionic lines here are all scalar.

To understand the consequences, we write the tensorial part of the scattering amplitude of a ladder scalar line box diagram [Fig. 15(a)] and the corresponding crossed scalar line box diagram [Fig. 15(b)]:

For the left diagram we have

$$\begin{aligned}\mathcal{M}_1 = \bar{u}(k_1)\bigg[\int \frac{dq^4}{(2\pi)^4} i\lambda_{3ki}\frac{1+\gamma_5}{2}\frac{i(\not{q}+m_{\ell_i})}{q^2-m^2_{\ell_i}} i\lambda_{3ji} \\ \times \frac{1-\gamma_5}{2}u(p_1)\frac{i}{(p_1-q)^2-m^2_{\tilde{\ell}_{L,j}}}\frac{i}{(k_1-q)^2-m^2_{\tilde{\ell}_{L,k}}} \\ \times \bar{u}(k_2)i\lambda_{mk1}\frac{1-\gamma_5}{2}\frac{i(\not{p}_2+\not{p}_1-\not{q}+m_{\nu_m})}{q^2-m^2_{\nu_m}} \\ \times i\lambda_{mj1}\frac{1+\gamma_5}{2}\bigg]u(p_2), \qquad (52)\end{aligned}$$

while for the right diagram we have

$$\begin{aligned}\mathcal{M}_2 = \bar{u}(k_1)\bigg[\int \frac{dq^4}{(2\pi)^4} i\lambda_{3ji}\frac{1+\gamma_5}{2}\frac{i(\not{q}+m_{\ell_i})}{q^2-m^2_{\ell_i}} i\lambda_{3ki} \\ \times \frac{1-\gamma_5}{2}u(p_1)\frac{i}{(p_1-q)^2-m^2_{\tilde{\ell}_{L,k}}}\frac{i}{(k_1-q)^2-m^2_{\tilde{\ell}_{L,j}}} \\ \times \bar{u}(k_2)i\lambda_{mk1}\frac{1-\gamma_5}{2}\frac{i(\not{p}_2-\not{k}_1+\not{q}+m_{\nu_m})}{q^2-m^2_{\nu_m}} i\lambda_{mj1} \\ \times \frac{1+\gamma_5}{2}\bigg]u(p_2). \qquad (53)\end{aligned}$$

Therefore, in the approximation of zero external legs ($p_1, p_2, k_1, k_2 = 0$), we have $\mathcal{M}_1 = -\mathcal{M}_2$. From a physical point of view, it is actually quite natural that such corrections cancel out when considering vanishing external legs, the Feynman box diagrams are antisymmetric in this case since scalar particles are exchanged and the sign of the ν_m neutrino impulsion is opposite.

V. IMPLICATIONS ON THE ELECTRON (ANTI-) NEUTRINO FLUXES

The consequence of adding $V_{\mu\tau}$ in the evolution equation of neutrinos in an astrophysical context was first studied in [36]. The authors, using approximations, demonstrate that the addition of such a term will imply a CP-violating phase (δ) dependence on the electron neutrino survival probability.

In this section, we analytically, without any approximation, show such dependence, using time discretization.[4] Note that this derivation is actually valid for any term contained in the interaction Hamiltonian which breaks the symmetry between mu and tau neutrinos. We focus here only on this particular term; therefore, this derivation does not need to include the neutrino-neutrino interaction term. Indeed, it has been analytically proven in [31] that, without $V_{\mu\tau}$, such a nonlinear term will induce

[4]Here we decided to work with wave functions and evolution operators for simplicity. Nevertheless, it is equivalent to the use of the matrix density formalism or the polarization vector as showed, for instance, in [19].

CP-violating only if there is a difference in the mu and tau neutrino fluxes emitted at the neutrinosphere.

A. The factorization

In a dense environment the neutrino evolution equations with one-loop correction to matter interactions are given by

$$i\frac{\partial}{\partial t}\begin{pmatrix}\Psi_e\\ \Psi_\mu\\ \Psi_\tau\end{pmatrix} = \left[U\begin{pmatrix}E_1 & 0 & 0\\ 0 & E_2 & 0\\ 0 & 0 & E_3\end{pmatrix}U^\dagger + \begin{pmatrix}V_c & 0 & 0\\ 0 & 0 & 0\\ 0 & 0 & V_{\mu\tau}\end{pmatrix}\right]\begin{pmatrix}\Psi_e\\ \Psi_\mu\\ \Psi_\tau\end{pmatrix}, \tag{54}$$

where Ψ_α denotes a neutrino in a flavor state $\alpha = e, \mu, \tau$, $E_{i=1,2,3}$, being the energies of the neutrino mass eigenstates, and U, the MNSP matrix. The neutrino interaction with matter is taken into account through an effective Hamiltonian which corresponds, at the tree level, to the diagonal matrix $H_m = \mathrm{diag}(V_c, 0, 0)$, where the $V_c(x) = \sqrt{2}G_F N_e(x)$ potential, due to the charged-current interaction, depends upon the electron density $N_e(x)$ (note that the neutral current interaction introduces an overall phase only). Following the derivation of [31,58], to obtain explicit relations between probabilities and the CP-violating phase, it is convenient to work within a new basis where a rotation by T_{23} is performed. In this basis, one can factorize the S matrix, defined by $\mathrm{diag}(1, 1, e^{i\delta})$, out of the Hamiltonian, so that

$$\begin{aligned} i\frac{\partial}{\partial t}\begin{pmatrix}\Psi_e\\ \tilde\Psi_\mu\\ \tilde\Psi_\tau\end{pmatrix} &= \tilde H_T(\delta)\begin{pmatrix}\Psi_e\\ \tilde\Psi_\mu\\ \tilde\Psi_\tau\end{pmatrix}\\ &= S\tilde H'_T(\delta)S^\dagger\begin{pmatrix}\Psi_e\\ \tilde\Psi_\mu\\ \tilde\Psi_\tau\end{pmatrix}\\ &= S\left[T^0_{13}T_{12}\begin{pmatrix}E_1 & 0 & 0\\ 0 & E_2 & 0\\ 0 & 0 & E_3\end{pmatrix}T^\dagger_{12}T^{0\dagger}_{13} + \begin{pmatrix}V_c & 0 & 0\\ 0 & s^2_{23}V_{\mu\tau} & -c_{23}s_{23}e^{i\delta}V_{\mu\tau}\\ 0 & -c_{23}s_{23}e^{-i\delta}V_{\mu\tau} & c^2_{23}V_{\mu\tau}\end{pmatrix}\right]\\ &\quad\times S^\dagger\begin{pmatrix}\Psi_e\\ \tilde\Psi_\mu\\ \tilde\Psi_\tau\end{pmatrix}, \end{aligned} \tag{55}$$

Contrary to the case where only tree-level matter interaction is considered, the S matrix does not commute with the matter Hamiltonian in the T_{23} basis which is

$$\begin{aligned}\tilde\psi_\mu &= \cos\theta_{23}\psi_\mu - \sin\theta_{23}\psi_\tau,\\ \tilde\psi_\tau &= \sin\theta_{23}\psi_\mu + \cos\theta_{23}\psi_\tau.\end{aligned} \tag{56}$$

This fact implies that

$$\tilde H_T(\delta) \neq S\tilde H_T(\delta = 0)S^\dagger, \tag{57}$$

and, therefore, that

$$\tilde U_m(\delta) \neq S\tilde U_m(\delta = 0)S^\dagger. \tag{58}$$

B. Consequence on the electron neutrino survival probability

Nevertheless, the factorization of the S matrices is always possible but the Hamiltonian $\tilde H'_T(\delta)$ will depend on δ. We can rewrite Eq. (55) in the evolution operator formalism to be

$$\begin{aligned} i\frac{\partial}{\partial t}\begin{pmatrix}A_{ee} & A_{\tilde\mu e} & A_{\tilde\tau e}e^{i\delta}\\ A_{e\tilde\mu} & A_{\tilde\mu\tilde\mu} & A_{\tilde\tau\tilde\mu}e^{i\delta}\\ A_{e\tilde\tau}e^{-i\delta} & A_{\tilde\mu\tilde\tau}e^{-i\delta} & A_{\tilde\tau\tilde\tau}\end{pmatrix} &= \tilde H'_T(\delta)\begin{pmatrix}A_{ee} & A_{\tilde\mu e} & A_{\tilde\tau e}e^{i\delta}\\ A_{e\tilde\mu} & A_{\tilde\mu\tilde\mu} & A_{\tilde\tau\tilde\mu}e^{i\delta}\\ A_{e\tilde\tau}e^{-i\delta} & A_{\tilde\mu\tilde\tau}e^{-i\delta} & A_{\tilde\tau\tilde\tau}\end{pmatrix}. \end{aligned} \tag{59}$$

Defining the Hamiltonian $\tilde H'_T(\delta)$ by[5]

$$\tilde H'_T(\delta) = \begin{pmatrix}a & b & c\\ b & d & (e - ge^{i\delta})\\ c & (e - ge^{-i\delta}) & f\end{pmatrix}, \tag{60}$$

we can rewrite the evolution equations for the amplitudes of the first column of the evolution operator, which corresponds to the creation of an electron neutrino ν_e initially:

$$\begin{aligned} i\frac{d}{dt}A_{ee} &= aA_{ee} + bA_{e\tilde\mu} + cA_{e\tilde\tau}e^{-i\delta},\\ i\frac{d}{dt}A_{e\tilde\mu} &= bA_{ee} + dA_{e\tilde\mu} + (e - ge^{i\delta})A_{e\tilde\tau}e^{-i\delta},\\ i\frac{d}{dt}A_{e\tilde\tau}e^{-i\delta} &= cA_{ee} + (e - ge^{i\delta})A_{e\tilde\mu} + fA_{e\tilde\tau}e^{-i\delta}. \end{aligned} \tag{61}$$

Similarly, we can write the same equation for the amplitudes $B_{\alpha\beta}$ when δ is taken to be zero and look at the difference between the amplitudes that depend on δ and those which do not. The basic idea here is to prove that, because of the one-loop correction term $V_{\mu\tau}$, the function $(A_{ee} - B_{ee})$ cannot remain as a zero function by showing that its derivative is nonzero;

[5]Note that the terms a, b, c, d, e, f, and g are real.

$$\begin{aligned}
i\frac{d}{dt}(A_{ee}-B_{ee}) &= a(A_{ee}-B_{ee})+b(A_{e\tilde{\mu}}-B_{e\tilde{\mu}})\\
&\quad + c(A_{e\tilde{\tau}}e^{-i\delta}-B_{e\tilde{\tau}}),\\
i\frac{d}{dt}(A_{e\tilde{\mu}}-B_{e\tilde{\mu}}) &= b(A_{ee}-B_{ee})+d(A_{e\tilde{\mu}}-B_{e\tilde{\mu}})\\
&\quad + e(A_{e\tilde{\tau}}e^{-i\delta}-B_{e\tilde{\tau}})+g(A_{e\tilde{\tau}}-B_{e\tilde{\tau}}),\\
i\frac{d}{dt}(A_{e\tilde{\tau}}e^{-i\delta}-B_{e\tilde{\tau}}) &= c(A_{ee}-B_{ee})+e(A_{e\tilde{\mu}}-A_{e\tilde{\mu}})\\
&\quad + f(A_{e\tilde{\tau}}e^{-i\delta}-B_{e\tilde{\tau}})\\
&\quad - g(A_{e\tilde{\mu}}e^{-i\delta}-B_{e\tilde{\mu}}).
\end{aligned} \tag{62}$$

Let us now take a closer look at Eqs. (62). The initial condition we are interested in, namely, a ν_e created initially means that initially the amplitudes A and B are

$$\begin{pmatrix}\Psi_e\\ \Psi_\mu\\ \Psi_\tau\end{pmatrix}=\begin{pmatrix}1\\0\\0\end{pmatrix}\Rightarrow\begin{pmatrix}A_{ee}\\ A_{e\tilde{\mu}}\\ A_{e\tilde{\tau}}e^{-i\delta}\end{pmatrix}=\begin{pmatrix}B_{ee}\\ B_{e\tilde{\mu}}\\ B_{e\tilde{\tau}}\end{pmatrix}=\begin{pmatrix}1\\0\\0\end{pmatrix}. \tag{63}$$

When $g=0$ ($V_{\mu\tau}=0$), it is easy to see that inserting the initial conditions into Eqs. (62) will imply that the functions $f_e=A_{ee}-B_{ee}$, $f_\mu=A_{e\tilde{\mu}}-B_{e\tilde{\mu}}$, and $f_\tau=A_{e\tilde{\tau}}e^{-i\delta}-B_{e\tilde{\tau}}$ will be equal to zero. By discretizing time we see, by recurrence, that if those functions are zero at the beginning, they will be equal to zero at all times. But when $g\neq 0$ ($V_{\mu\tau}\neq 0$) we have to look also at the evolution of the functions $\hat{f}_\mu=A_{e\tilde{\mu}}e^{-i\delta}-B_{e\tilde{\mu}}$ and $\hat{f}_\tau=A_{e\tilde{\tau}}-B_{e\tilde{\tau}}$. Their respective evolution equation can be easily derived from Eq. (61) to yield

$$\begin{aligned}
i\frac{d}{dt}(A_{e\tilde{\mu}}e^{-i\delta}-B_{e\tilde{\mu}}) &= b(A_{ee}e^{-i\delta}-B_{ee})+d(A_{e\tilde{\mu}}e^{-i\delta}\\
&\quad - B_{e\tilde{\mu}})+e(A_{e\tilde{\tau}}e^{-2i\delta}-B_{e\tilde{\tau}})\\
&\quad + g(A_{e\tilde{\tau}}e^{-i\delta}-B_{e\tilde{\tau}}),
\end{aligned} \tag{64}$$

$$\begin{aligned}
i\frac{d}{dt}(A_{e\tilde{\tau}}-B_{e\tilde{\tau}}) &= c(A_{ee}e^{i\delta}-B_{ee})+e(A_{e\tilde{\mu}}e^{i\delta}-A_{e\tilde{\mu}})\\
&\quad + f(A_{e\tilde{\tau}}-B_{e\tilde{\tau}})-g(A_{e\tilde{\mu}}-B_{e\tilde{\mu}}).
\end{aligned} \tag{65}$$

Initially, the derivatives are

$$\begin{aligned}
i\frac{d}{dt}(A_{e\tilde{\mu}}e^{-i\delta}-B_{e\tilde{\mu}})(t=0) &= i\frac{d}{dt}\hat{f}_\mu(t=0)\\
&= b(e^{-i\delta}-1),\\
i\frac{d}{dt}(A_{e\tilde{\tau}}-B_{e\tilde{\tau}})(t=0) &= i\frac{d}{dt}\hat{f}_\tau(t=0)\\
&= c(e^{i\delta}-1).
\end{aligned} \tag{66}$$

We just proved that since the functions $\hat{f}_\mu$ and $\hat{f}_\tau$ are different from the constant zero function, the functions f_μ and f_τ will not be zero as well. But does it imply that the function f_e is nonzero at all time? No, because the contributions from $\hat{f}_\mu$ and $\hat{f}_\tau$ could cancel in the evolution equation (62) of f_e. To precisely study the evolution of f_e, we discretize time such as $t=N*\Delta t$ with $N\in\mathbb{N}$ and

$$f_\alpha(t+\Delta t)=f_\alpha(t)+\Delta t\times\frac{df_\alpha}{dt}(t), \tag{67}$$

where $\alpha=e,\mu,\tau$. Using Eqs. (62) and (67) we see that, at $t=\Delta t$,

$$\hat{f}_\mu(\Delta t)=\frac{b(e^{-i\delta}-1)}{i}\Delta t,\qquad \hat{f}_\tau(\Delta t)=\frac{c(e^{i\delta}-1)}{i}\Delta t, \tag{68}$$

which implies that, at $t=2\Delta t$

$$\begin{aligned}
f_\mu(2\Delta t) &= -gc(e^{i\delta}-1)\Delta^2 t,\\
f_\tau(2\Delta t) &= gb(e^{-i\delta}-1)\Delta^2 t,
\end{aligned} \tag{69}$$

leading at $t=3\Delta t$,

$$\begin{aligned}
f_e(3\Delta t) &= \frac{1}{i}(gbc(e^{-i\delta}-1)-gbc(e^{i\delta}-1))\Delta^3 t\\
&= \frac{1}{i}gbc(e^{-i\delta}-e^{i\delta})\Delta^3 t=-2gbc\sin\delta\Delta^3 t.
\end{aligned} \tag{70}$$

This last formula proves that the function f_e is not the constant zero function when $\delta\neq 0$,[6] therefore $A_{ee}\neq B_{ee}$ and consequently, for $V_{\mu\tau}\neq 0$:

$$P(\nu_e\to\nu_e,\delta\neq 0)\neq P(\nu_e\to\nu_e,\delta=0). \tag{71}$$

Therefore, when δ is nonzero, it has an influence on the value of $P(\nu_e\to\nu_e,\delta)$. The luminosity of a neutrino emitted initially as a flavor α is

$$L_{\nu_{\underline{\alpha}}}(r,E_\nu)=\frac{L^0_{\nu_{\underline{\alpha}}}}{T^3_{\nu_{\underline{\alpha}}}\langle E_{\nu_{\underline{\alpha}}}\rangle F_2(\eta)}\frac{E^2_{\nu_{\underline{\alpha}}}}{1+\exp(E_{\nu_{\underline{\alpha}}}/T_{\nu_{\underline{\alpha}}}-\eta)}, \tag{72}$$

where $F_2(\eta)$ is the Fermi integral, $L^0_{\nu_{\underline{\alpha}}}$ and $T_{\nu_{\underline{\alpha}}}$ are the luminosity and temperature at the neutrinosphere. The ν_e and $\bar{\nu}_e$ fluxes will depend on δ even when the luminosities $L_{\nu_{\underline{\mu}}}$ and $L_{\nu_{\underline{\tau}}}$ are taken equal at the neutrinosphere:

$$\begin{aligned}
\phi_{\nu_e}(\delta) &= L_{\nu_{\underline{e}}}P(\nu_e\to\nu_e,\delta)+L_{\nu_{\underline{\mu}}}(P(\nu_\mu\to\nu_e)\\
&\quad + P(\nu_\tau\to\nu_e)),\\
&= L_{\nu_{\underline{e}}}P(\nu_e\to\nu_e,\delta)+L_{\nu_{\underline{\mu}}}(1-P(\nu_e\to\nu_e,\delta)),\\
&= (L_{\nu_{\underline{e}}}-L_{\nu_{\underline{\mu}}})P(\nu_e\to\nu_e,\delta)+L_{\nu_{\underline{\mu}}}.
\end{aligned} \tag{73}$$

This analytical derivation proves that, if the dependence on

[6]Note that with such a formula, f_e is also equal to zero when $\delta=\pi$, but going to the forth step will show, after a tedious but straightforward calculation, that f_e is nonzero even when $\delta=\pi$.

δ of the evolution operator cannot be factorized then the electron neutrino survival probability depends on δ. It is valid for any astrophysical environment such as a supernova, or the Sun. Nevertheless, this implication had been observed numerically. We can easily generalize this derivation to other interactions that would distinguish ν_μ from ν_τ like, for instance, nonstandard neutrino interaction [59]. Therefore, we can state that as soon as the medium effect on ν_μ and on ν_τ is not the same, effects of the CP-violating phase on the electron neutrino (and antineutrino) fluxes will appear.

VI. DISCUSSIONS

In the previous sections we have studied the SUSY radiative corrections to supernova neutrino scattering with and without R-parity breaking. In the second part, we have analyzed the implications on the electron (anti) neutrino fluxes by considering an analytical derivation of the CP-violating phase dependence on the electron neutrino survival probability. In this section, we intend to discuss the model considered in this paper and to replace it in a more general context.

A. Concerning the model

We worked in the NMSSM which is a more promising supersymmetric model than the MSSM for experimental and theoretical reasons. In our model, we consider all R-parity breaking terms. These interactions are controlled by the following parameters: μ_i, λ_i, λ_{ijk}, λ'_{ijk}, and λ''_{ijk}. In general, the tree-level contributions will dominate all the one-loop R-parity breaking contributions to neutrino indices of refraction.

For instance, if we assume λ_{ijk} or λ'_{ijk} to be dominant and of the maximal order of magnitude $O(10^{-1})$, we showed that the $\not{R}_P$ contributions can be bigger than the R-parity conserved contributions. On the other hand, if we make the hypothesis that λ_{ijk}, λ'_{ijk}, and λ''_{ijk}, are of the same order of magnitude, the $\not{R}_P$ contributions will often be negligible.

In our framework, we have only considered the NMSSM's fields content, for instance neutrinos are just associated with left-handed fields. Here, two neutrino masses are generated at the tree level by considering the two terms μ_i and λ_i among all the R-parity breaking terms. Note that neutrino masses can be generated at the tree level in different models such as models with seesaw mechanisms [53,54] even in the limit of massless neutrinos. In these models, new right-handed neutrino fields are added and new couplings are induced between the existing fields and the new ones and between the right-handed fields.[7]

In the literature, there exist some specific models which allow us to generate neutrino masses with R-parity breaking. The most popular one is the pure bilinear model (with only $\mu_i\hat{H}_u\hat{L}_i$) in the MSSM framework where only one neutrino mass is generated at the tree level [55]. If we consider this case, we can see that the only nonvanishing term is the tree-level correction $\Delta\rho_c(\chi^0)$ of Eq. (30). This term is of the order of magnitude $O(10^{-15})$, and thus always negligible with respect to R-parity conserved terms. The model we consider in this paper is an extension of the pure bilinear case in the NMSSM framework. It can lead to non-negligible corrections as seen before.

Throughout the paper, we have studied how supersymmetry does affect the neutrino indices of refraction. In the standard model, they are found to be small: $\varepsilon_{\mathrm{SM}} \simeq 5.4 \times 10^{-5}$ [8]. When we consider the R-parity conserved supersymmetric contributions, we have shown in the regions of the parameters' space considered that ε can go up to 2×10^{-2} and can even be negative whereas it was previously found to be up to 10^{-3} in the MSSM [9]. This is consistent with the fact that the parameters' space in the NMSSM is larger than in the MSSM.

B. Concerning the implications on the electron (anti-)neutrino fluxes

In the previous section, we have shown that when $V_{\mu\tau}$ breaks the symmetry between muon and tau neutrinos, it creates a CP-violating phase dependence for the electron (anti)neutrino survival probabilities and consequently on the electron (anti)neutrino fluxes. This derivation is valid for any dense environment such as a core-collapse supernova or the Sun. In the supernova environment, such a phenomenon was numerically observed in [58]. The addition of the nonlinear neutrino-neutrino interaction induces larger effects on the electron neutrino flux up to a level of 10% when $\delta = \pi$ inside the supernova [31] for a standard model value of ε. The fact that in the SUSY framework, $V_{\mu\tau}$ can be up to a factor $2 \times 10^{-2} V_e$ will logically yield even larger effects. Note that to determine the precise size of these effects, a numerical approach is necessary and beyond the scope of this paper. Moreover, in this environment, the density is sufficiently high that neutrinos encounter not only the so-called high resonance associated with Δm^2_{13} and the low resonance associated with Δm^2_{12}, but also the $\mu - \tau$ resonance whose precise conditions depend on the hierarchy [60]. The importance of such a matter interaction correction term has been investigated in [27,29] showing that such resonance could influence the electron neutrino flux, when taking into account the neutrino-neutrino interaction. Consequently, an important ε coming from SUSY radiative corrections could lead to important effects on the electron neutrino probability because of the interplay between this $\mu - \tau$ resonance and the $\nu - \nu$ interaction depending on the sign of ε and the octant of θ_{23}, even for a zero value of δ.

In the Sun environment, where no $\nu - \nu$ interaction is present, the impact of $V_{\mu\tau}$ with or without a nonzero

[7]The latter couplings may break the R-parity.

CP-violating phase has been studied in [36]. The authors claim that the correction term induced a small effect on the flavor conversion probabilities of the order of ε. Therefore, in the SUSY framework, effects could be up to the order of several percents if δ is not too small. Though identifying precisely the effects of the *CP*-violating phase in the neutrino signal could be difficult, it would be interesting to investigate such a possibility in detail.

VII. CONCLUSIONS

In this paper, we have investigated the radiative correction on the $\mu - \tau$ neutrino indices of refraction coming from beyond standard physics. In the NMSSM, we have shown that the sign of $V_{\mu\tau}$ depends upon the hierarchy of the sleptons masses and therefore could be negative contrary to the standard model case. After writing and adding a subroutine to a low-energy code, taking into account all current constraints on SUSY, we showed that ε can increase up to the order of 2×10^{-2} depending on the supersymmetric parameters. Such value could be highly important in the calculation of neutrino fluxes from core-collapse supernovae as it can induce sizeable effects upon the electron (anti)neutrino fluxes. In a second part we have calculated all contributions from R-parity breaking interactions on the radiative corrections $V_{\mu\tau}$. Taking into account such interactions, we showed that NMSSM distinguishes from MSSM in this case and brings new possible contributions. The next step in this type of calculation would be to see the consequences of theses values of $V_{\mu\tau}$ on the supernova neutrino fluxes and to use it in order to survey the supersymmetric parameter space [61]. Second, we would have to calculate corrections with gravitino loops and all contributions from R-parity breaking interactions. Another interesting possibility would be to calculate the radiative corrections for the neutrino-neutrino interaction. Such a calculation has been recently done in the standard model [62] and the SUSY framework could yield a potentially much bigger effect. Finally, as an application for $V_{\mu\tau}$ we demonstrated that the inclusion of such a term implies that the electron (anti) neutrino survival probability, and consequently the electron (anti)neutrino fluxes, will depend upon δ. The consequences of such dependence and the fact that $V_{\mu\tau}$ can be up to $2 \times 10^{-2} V_e$ will be studied in a future work.

ACKNOWLEDGMENTS

The authors are grateful to S. Friot for his enthusiasm and encouragement during the realization of this work and for useful discussion. They also want to thank F. Domingo, J. Kneller, and S. Descotes-Genon for fruitful discussions. Finally, they thank A. Mirizzi, P. D. Serpico, and J. Kneller for the careful reading of the manuscript.

[1] L. Wolfenstein, Phys. Rev. D **17**, 2369 (1978); **20**, 2634 (1979).
[2] S. P. Mikheev and A. Y. Smirnov, Nuovo Cimento Soc. Ital. Fis. C **9**, 17 (1986).
[3] R. Davis, Phys. Rev. Lett. **12**, 303 (1964).
[4] S. Sarantakos, A. Sirlin, and W. J. Marciano, Nucl. Phys. **B217**, 84 (1983).
[5] L. M. Sehgal, Phys. Lett. **162B**, 370 (1985).
[6] P. Langacker, J. P. Leveille, and J. Sheiman, Phys. Rev. D **27**, 1228 (1983).
[7] R. R. Lewis, Phys. Rev. D **21**, 663 (1980).
[8] F. J. Botella, C. S. Lim, and W. J. Marciano, Phys. Rev. D **35**, 896 (1987).
[9] E. Roulet, Phys. Lett. B **356**, 264 (1995).
[10] E. K. Akhmedov, C. Lunardini, and A. Y. Smirnov, Nucl. Phys. **B643**, 339 (2002).
[11] J. T. Pantaleone, Phys. Lett. B **287**, 128 (1992).
[12] G. Sigl and G. Raffelt, Nucl. Phys. **B406**, 423 (1993).
[13] S. Samuel, Phys. Rev. D **48**, 1462 (1993).
[14] Y. Z. Qian and G. M. Fuller, Phys. Rev. D **51**, 1479 (1995).
[15] G. Sigl, Phys. Rev. D **51**, 4035 (1995).
[16] S. Pastor, G. G. Raffelt, and D. V. Semikoz, Phys. Rev. D **65**, 053011 (2002).
[17] S. Pastor and G. Raffelt, Phys. Rev. Lett. **89**, 191101 (2002).
[18] A. B. Balantekin and H. Yuksel, New J. Phys. **7**, 51 (2005).
[19] H. Duan, G. M. Fuller, and Y. Z. Qian, Phys. Rev. D **74**, 123004 (2006).
[20] H. Duan, G. M. Fuller, J. Carlson, and Y. Z. Qian, Phys. Rev. D **74**, 105014 (2006).
[21] S. Hannestad, G. G. Raffelt, G. Sigl, and Y. Y. Y. Wong, Phys. Rev. D **74**, 105010 (2006); **76**, 029901(E) (2007).
[22] A. B. Balantekin and Y. Pehlivan, J. Phys. G **34**, 47 (2007).
[23] H. Duan, G. M. Fuller, J. Carlson, and Y. Z. Qian, Phys. Rev. Lett. **97**, 241101 (2006).
[24] G. L. Fogli, E. Lisi, A. Marrone, and A. Mirizzi, J. Cosmol. Astropart. Phys. 12 (2007) 010.
[25] G. G. Raffelt and A. Y. Smirnov, Phys. Rev. D **76**, 081301 (2007); **77**, 029903(E) (2008).
[26] G. G. Raffelt and A. Y. Smirnov, Phys. Rev. D **76**, 125008 (2007).
[27] A. Esteban-Pretel, S. Pastor, R. Tomas, G. G. Raffelt, and G. Sigl, Phys. Rev. D **77**, 065024 (2008).
[28] H. Duan, G. M. Fuller, J. Carlson, and Y. Z. Qian, Phys. Rev. Lett. **100**, 021101 (2008).
[29] H. Duan, G. M. Fuller, and Y. Z. Qian, Phys. Rev. D **77**, 085016 (2008).
[30] B. Dasgupta and A. Dighe, Phys. Rev. D **77**, 113002 (2008).
[31] J. Gava and C. Volpe, Phys. Rev. D **78**, 083007 (2008).

[32] A. Esteban-Pretel, S. Pastor, R. Tomas, G. G. Raffelt, and G. Sigl, Phys. Rev. D **76**, 125018 (2007).
[33] A. Esteban-Pretel, A. Mirizzi, S. Pastor, R. Tomas, G. G. Raffelt, P. D. Serpico, and G. Sigl, Phys. Rev. D **78**, 085012 (2008).
[34] J. Gava, J. Kneller, C. Volpe, and G. C. McLaughlin, Phys. Rev. Lett. **103**, 071101 (2009)..
[35] S. Galais, J. Kneller, C. Volpe, and J. Gava, arXiv:0902.0317.
[36] H. Minakata and S. Watanabe, Phys. Lett. B **468**, 256 (1999).
[37] J. Wess and J. Bagger, *Supersymmetry and Supergravity* (Princeton University Press, Princeton, 1992), 2nd ed.
[38] J. E. Kim and H. P. Nilles, Phys. Lett. **138B**, 150 (1984).
[39] M. Maniatis, arXiv:hep-ph/0906.0777v1; U. Ellwanger *et al.*, Z. Phys. C **67**, 665 (1995); Nucl. Phys. **B492**, 21 (1997); U. Ellwanger and C. Hugonie, Eur. Phys. J. C **25**, 297 (2002); U. Ellwanger *et al.*, J. High Energy Phys. 07 (2005) 041; U. Ellwanger and C. Hugonie, Phys. Lett. B **623**, 93 (2005).
[40] A. Abada and G. Moreau, J. High Energy Phys. 08 (2006) 044; A. Abada, G. Bhattacharyya, and G. Moreau, Phys. Lett. B **642**, 503 (2006).
[41] S. Friot, D. Greynat, and E. De Rafael, Phys. Lett. B **628**, 73 (2005).
[42] J. Gunion and H. E. Haber, Nucl. Phys. **B272**, 1 (1986); H. Haber and G. L. Kane, Phys. Rep. **117**, 75 (1985).
[43] U. Ellwanger, J. F. Gunion, and C. Hugonie, J. High Energy Phys. 02 (2005) 066; U. Ellwanger, http://www.th.u-psud.fr/NMHDECAY/nmssmtools.html.
[44] S. Bertolini, F. Borzumati, A. Masiero, and G. Ridolfi, Nucl. Phys. **B353**, 591 (1991).
[45] J. Rosiek, arXiv:hep-ph/9511250v3.
[46] S. Dimopoulos and G. Giudice, Nucl. Phys. **B454**, 59 (1995).
[47] U. Ellwanger and C. Hugonie, Comput. Phys. Commun. **177**, 399 (2007).
[48] U. Ellwanger, C.-C. Jean-Louis, and A. M. Teixeira, J. High Energy Phys. 05 (2008) 044.
[49] E. Roulet, Phys. Rev. D **44**, R935 (1991).
[50] C.-C. Jean-Louis and G. Moreau, arXiv:0911.3640v1.
[51] M. Chemtob and P. N. Pandita, Phys. Rev. D **73**, 055012 (2006).
[52] M. Chemtob, Prog. Part. Nucl. Phys. **54**, 71 (2005).
[53] R. N. Mohapatra and J. W. F. Valle, Phys. Rev. D **34**, 1642 (1986).
[54] Pei-Hong Gu, M. Hirsch, Utpal Sarkar, and J. W. F. Valle, Phys. Rev. D **79**, 033010 (2009);
[55] F. Takayama and M. Yamaguchi, arXiv:hep-ph/0005296v1.
[56] P. S. Amanik, G. M. Fuller, and B. Grinstein, Astropart. Phys. **24**, 160 (2005).
[57] R. Barbier *et al.*, Phys. Rep. **420**, 1 (2005).
[58] A. B. Balantekin, J. Gava, and C. Volpe, Phys. Lett. B **662**, 396 (2008).
[59] A. Esteban-Pretel, R. Tomas, and J. W. F. Valle, Phys. Rev. D **76**, 053001 (2007).
[60] J. P. Kneller and G. C. McLaughlin, Phys. Rev. D **80**, 053002 (2009).
[61] J. Gava and C.-C. Jean-Louis, arXiv:0912.5206v1.
[62] A. Mirizzi, S. Pozzorini, G. G. Raffelt, and P. D. Serpico, J. High Energy Phys. 10 (2009) 020.